HEAT TRANSFER STUDIES IN SWIRLING FLOW IN LONG TUBE

A Dissertation
submitted in partial fulfilment of the
~~requirements for the award of the Degree~~
of
MASTER OF ENGINEERING
in
CHEMICAL ENGINEERING
(PALNT AND EQUIPMENT DESIGN)

By

NARINDER KUMARI

DEPARTMENT OF CHEMICAL ENGINEERING
UNIVERSITY OF ROORKEE
ROORKEE (INDIA)
August, 1974

CERTIFICATE

Certified that the thesis entitled 'HEAT TRANSFER STUDIES IN SWIRLING FLOW IN LONG TUBE' which is being submitted by Miss Harinder Kumari in partial fulfilment of the requirements for the award of the degree of MASTER OF ENGINEERING IN CHEMICAL ENGINEERING (Equipment and Plant Design) of University of Roorkee, is a record of candidate's own work carried out by her under the supervision and guidance of the undersigned. The matter embodied in this thesis has not been submitted for award of any other degree or diploma.

This is further certified that she has worked for a period of about seven months for preparing this thesis at this university.

(B.D.Sharma)

Reader,
Chemical Engineering Dept.
University of Roorkee,
Roorkee.

(D.V.Pangarkar) 14/8/74

Associate Professor
Chemical Engineering Department
University of Roorkee,
ROORKEE

Dated: August 22, 1974.

ABSTRACT

A heat-transfer model for swirling flow in long tube has been proposed. To check the validity of the proposed model, equipment for study of heat transfer to swirling flow in long tube was set up. This consisted of a swirl chamber machined from 25 mm thick perspex plates. The plates were held together by four 6 mm. dia rods. To this swirl chamber inside tube of the double pipe heat exchanger was fixed by stuffing box arrangement. The liquid was heated by means of steam. Calibrated copper constantan thermocouples were used for measuring the liquid and steam temperatures.

The experimental data for water and three different dilutions of glycerine-water mixture were taken. The values of heat transfer coefficients for these liquids were found to increase with the increase in the velocity. Effects of variation of tangential inlet velocity, tangential inlet diameters, and kinematic viscosity of the fluid at different steam temperatures were studied. The performance of the swirl flow heat exchanger has been compared with that of an axial flow heat exchanger. It has been observed that the overall heat transfer coefficients in swirl flow are 100 percent higher than those obtained in the case of axial flow.

90 percent of the experimental data points lie

within ± 25%. in the following theoretical model

$$Nu = 0.023\left(\frac{D_H G}{\mu}\right)^{0.8}\left(\frac{C_p \mu}{k}\right)^{1/3}\left[1 + \frac{(v_z \alpha r_s / r_w)^2}{450\ \bar{u}^2 f}\right]^{1/2}\left(\frac{D}{D_H}\right)\left(\frac{\mu_B}{\mu_w}\right)^{0.36}$$

The physical properties used in the dimensionless groups were taken at the average temperature of the liquid.

ACKNOWLEDGEMENTS

Many persons have contributed either directly or indirectly to this thesis; I would like to mention some of them by name:

Dr. P.D.Panesar, Associate Professor and Dr.B.D.Sharma, Reader of Chemical Engineering Department, University of Roorkee, Roorkee deserve many thanks for their constant encouragement and invaluable guidance during the preparation of this thesis.

Dr. B.S.Varshney, Professor, Chemical Engineering Department, University of Roorkee, Roorkee enlightened me with informative discussions and suggestions. I am indebted to him.

Dr. N.Gopal Krishna, Professor and Head, Department of Chemical Engineering, University of Roorkee, Roorkee provided me necessary laboratory and other facilities. I sincerely thank him for this.

Mr. N.C.Bansal, my classmate deserves my warmest thanks for helping me in the experimental work.

Special thanks are due to the non-teaching staff of the Department who were very cooperative and readily helped me throughout this work.

Narinder Kumar

CONTENTS

LIST OF FIGURES

NOMENCLATURE

a, b	width of annulus	m
A	area	m^2
C_p	specific heat	K Cal/kg °C
D	inside tube diameter	m
D_H	hydraulic diameter	m
d	air core diameter	m
G_c	conversion factor	$\frac{kg\ m}{kg_f\ sec^2}$
G	mass velocity	$\frac{kg}{m^2.hr}$
H	helical pitch	m
h_i	liquid film heat transfer coefficient	K Cal/hr.m^2.°C
h_o	heat transfer coefficient of steam	K Cal/hr.m^2.°C
k	thermal conductivity	K Cal/hr.m.°C
L_o	length of swirl	m
m	mass flow rate	kg/sec.
q	heat flux per unit area	K Cal/hr.m^2
r	air core radius	m
R	tube radius	m
T	temperature	°C
ΔT	temperature difference	°C
ΔT_m	log mean temperature difference	°C
$\bar{u}$	mean axial velocity	m/sec.
u	axial velocity	m/sec.

LIST OF TABLES

NOMENCLATURE

a, b	width of annulus	□
A	area	$□^2$
C_p	specific heat	KCal/kg°C
D	inside tube diameter	□
D_H	hydraulic diameter	□
d	air core diameter	□
G_c	conversion factor	$\frac{□}{□_F}\ \frac{□□}{□□□^2}$
G	mass velocity	$\frac{kg}{□^2.hr}$
H	helical pitch	□
h_i	liquid film heat transfer coefficient	KCal/hr.$□^2$°C
h_o	heat transfer coefficient of steam	KCal/hr.$□^2$°C
k	thermal conductivity	KCal/hr.□.°C
L_o	length of swirl	□
m	mass flow rate	kg/sec.
q	heat flux per unit area	KCal/hr.$□^2$
r	aircore radius	□
R	tube radius	□
T	temperature	°C
ΔT	temperature difference	°C
ΔT_m	log mean temperature difference	°C
$\bar{u}$	mean axial velocity	□/sec.
u	axial velocity	□/sec.

u^*	shear velocity $= \sqrt{\tau_w/\rho} = \bar{u}\sqrt{f/2}$	m/sec
V	velocity at the tangential entry	m/sec
V_o	actual velocity of liquid in tube	m/sec
V_θ	velocity in tangential coordinate direction	m/sec
y	distance from tube wall	m
δ	boundary layer thickness	m
μ	viscosity	kg/m.hr.
ν	kinematic viscosity	m^2/sec
ρ	density	gm/cm^3
τ	shear stress	gm_f/cm^2
Γ	circulation constant	cm^2/sec

Dimensionless Groups

f	Fanning friction factor	$\left(\frac{\Delta P}{\rho}\right)_T \frac{D_H \rho}{L_o V_e^2}$
f'	equivalent friction factor defined by eqn.3.11	
Nu	Nusselt Number	hD_H/k
Pr	Prandtl Number	$c_p\mu/k$
Re	Reynolds number	$D_H \bar{u}\, \rho/\mu$
St	Stanton Number	$h/\rho\, \bar{u} c_p$
N_{Ta}	Taylor Number	$\sqrt{d/r_1}\, \frac{\omega r_1 d}{\nu}$
u^+	Dimensionless velocity	u/u^*
y^+	dimensionless distance from wall	yu^*/ν

Subscripts

a	axial component
b	evaluated at bulk temperature

i	tube test section inlet condition
o	tube test section outlet condition
r	radial component
s	evaluated in swirl chamber
t	tangential component
T	total
v	vapour
w	evaluated at tube wall

CHAPTER I

INTRODUCTION

The overall heat transfer coefficient defines the intensity of heat transfer from one fluid to another through a wall separating them and is numerically equal to the quantity of heat passing through unit area of wall surface in unit time at a temperature difference of $1^{\circ}C$. It depends upon the film coefficient on the liquid side, the thermal conductance and thickness of tube, the amount of scale and dirt on the tube and the film coefficient on the steam side.

The resistance of the tube is small in comparison to the sum of the resistances of the both film coefficients and is usually neglected. For the new tubes dirt factor is neglected. In a system where heat is being transferred from condensing steam to water, the liquid film provides the major resistance so the heat transfer coefficient of condensing steam is very high. The performance of the heat exchanger can be improved by increasing the liquid film coefficient by some means.

The major resistance to heat transfer between solid boundaries and turbulent fluids is the laminar sublayer adjacent to the wall. The resistance of this laminar layer is proportional to its thickness, and any decrease in

resistance of this thickness will result in a comparable increase in the rate of heat transfer between the wall and the fluid.

Various research workers have tried to reduce the thickness of laminar sublayer by different methods. These can be grouped as under:

(i) By increasing the intensity and scale of the turbulence of the flowing stream. This is done by placing turbulence promoters, usually spiral tapes or strips in the conduit. They have the effect of increasing not only the rate of heat transfer but also the resistance to flow; so actually the heat transferred per unit of power expended may not be changed(10).

(ii) By increasing the turbulence of the flowing stream by vibrations or pulsations. In this method the liquid is supplied to tube by a reciprocating pump. The pulsations from the pump bring about a considerable increase in heat-transfer coefficient.

(iii) By generating swirling motion inside the tube. The swirl in a flowing stream can be achieved by:

(a) mechanical rotation of the pipe through which liquid is flowing.

(b) putting twisted tapes inside the pipe through which the liquid is flowing.

(c) Forcing the liquid into the tube through tangential inlets at the inner surface of the tube.

(d) Forcing the liquid through a swirl chamber installed at the upflow of the inner tube.

The relative merits and demerits of producing swirling flow have been discussed by Sharma et al.(9). It has been pointed out that it is most economical to produce swirling flow in long tubes by using a swirl chamber. The liquid film coefficients obtained by adopting different methods are given in Table 1.C1.

In the present investigation reversal in the swirling flow, generated by feeding liquid into a swirl chamber fixed to a long tube shall be eliminated by imposing ends of swirl ber to atmosphere. The aims of this work are:

(a) To predict a model of heat transfer for the above system.

(b) To check the validity of the proposed model by comparison with experimental data for different physical and dynamic parameters.

Table No.1.01 Heat Transfer Coefficients for Swirling Flow

Device used for creating Swirling Flow	h_i Kcal/hr.m^2.°C
Twisted Tape	3200-12000
Rotation of Inner Tube	1000-5000
Tangential Entry	3000-15000

CHAPTER 2

LITERATURE REVIEW

In any steam liquid heat transfer equipment the overall heat-transfer coefficient is normally controlled by the liquid film coefficient. Attempts have been made for the past few years to reduce the liquid boundary layer resistance by different techniques. The various techniques used are,

(1) Creation of turbulence by increasing the roughness of the surface in the axial flow or by increasing the velocity of the liquid.

(2) By inserting turbulence promoters in the tube.

(3) Increasing the turbulence of the flowing stream by vibrations or pulsations.

(4) By generating swirling flow inside the tube. This can be achieved by

(a) Rotating the tube through which the fluid is to flow.

(b) Inserting twisted tape in the tube.

(c) Injecting the fluid into the tube through tangential entries.

2.1 The condition of the surface in contact with the

fluid affects the heat-transfer coefficient for turbulent flow. The heat-transfer coefficient for a rough surface is higher than for a smooth surface because the roughness projections on the surface disturb the laminar sublayer. No general correlation showing the effect of wall roughness on the heat-transfer coefficient exists. There have been investigations in which one type of wall roughness was studied, but the results cannot be used to predict heat-transfer coefficients for other types of wall roughness.

Cope(10) made a study of the relation between heat transfer and friction loss in rough circular pipes. The pipes investigated were roughened by cutting both left-hand and right-hand threads in them, so that the surface was actually covered by small pyramids. Heat transfer coefficients in the form of dimensionless term $Nu\sqrt{Pr}$ and friction factor were both plotted versus the Reynolds number. The data indicated that rate of heat transfer is proportional to the roughness of the tubes.

Sams(10) gave a more general correlation dealing with wall roughness, who investigated heat transfer from tubes with square threads on their inner walls. The experimental data was represented within ± 15 percent by the relation

$$\left(\frac{h\,d_v}{k}\right)_{Pr=0.5} = 0.040\left(\frac{d_v u_z \rho}{\mu}\right)_{Pr=0.5}\left(\frac{c_p \mu}{k}\right)_{Pr=0.5} \quad \ldots (2.01)$$

Conditions:

(1) d_v = inside diameter of pipe.

(2) Properties evaluated at $t_{0.5}$

(3) $u_g^n = U\sqrt{f_r/2}$ where $f_r/2 = .036\left(\frac{b}{d_v}\right)^{0.5}\left(\frac{e}{d_v}\right)^{1.70}$

b = thread spacing,

U = thread thickness,

e = thread height,

(4) $500 < d_v u_g^n/\nu < 2 \times 10^4$.

2.2 Studies of the effect of turbulence promoters on the rate of heat transfer were made by Noyds(10), Seigel(10), and Colburn and King(10), who showed that turbulence promoters materially increase the rate of heat transfer. A variety of turbulence promoters were investigated. Seigel showed that heat-transfer coefficient for water in a tube with spiral wire is 150 percent higher than heat-transfer coefficient in an empty tube.

2.3 Turbulence of the flowing stream can be increased by vibrations or pulsations. Martinelli and Boelter(10) have studied the effect of vibrations on heat transfer from a tube. Voet and Taylor(10) determined heat-transfer coefficients for turbulent flow of water inside tubes to which water was supplied by a reciprocating pump. The pulsations from the pump brought about a considerable increase in the

heat-transfer coefficient over that predicted by Dittus and Boelter.

2.41 Kayo and Elgar(1) presented a comprehensive qualitative discussion of heat transfer between rotating cylinders. These authors presented a geometrical factor to treat the finite annulus width which must be used in the experimental work.

Becker(2) presented heat transfer data for air contained between horizontal concentric cylinders with an inner rotating cylinder with and without axial flow.

Bjorklund and Kayo(1) presented more comprehensive heat transfer data for air between concentric cylinders. These authors presented data for cylinders rotating in the same as well as opposite directions. Four ratios of of annulus to inner cylinder radius were used. The correlation proposed by them is

$$\frac{Nu}{Nu_t} = 0.175\ Ta^{1/2} \qquad 90 < Ta < 2000 \quad \ldots (2.02)$$

where Nu_t is the Nusselt number of annulus for stream line flow (conduction heat transfer) which is dependent only on geometry.

The heat transfer characteristics of water in rotational motion between horizontal concentric cylinders were studied by Hess and Kunn(1). Primary fluid motion due to rotation of the inner cylinders alone, and due to rotation of inner

cylinder with reverse flow caused by a cavity, was considered experimentally for two ratios of annulus width to inner cylinder radius. The results for two geometries and primary fluid dynamic conditions were correlated by a parameter related to the generalized stability parameter. In this study the heat flux was held constant and the temperature gradient was allowed to vary. The heat transfer results were given in terms of the parameter Nu/Nu_k

$$\frac{Nu}{Nu_k} = \frac{(T_i-T_o)_k}{(T_i-T_o)} \cdot \frac{\ln\left[\left(\frac{\delta}{r_i}\right)+1\right]}{\delta/a} \qquad \ldots (2.05)$$

Becker and Kayo(2) obtained experimental data for different types of flow in an annulus with an inner rotating cylinder. The heat transfer data were subdivided into the following two limiting cases and one general case.

Case A Axial flow with zero rotation.

Case B Rotation of inner cylinder with zero axial flow.

Case C General case of combined axial flow and rotation.

The heat transfer data from this study and of previous investigations were correlated in terms of Reynolds number and Taylor number over a wide range of these variables in terms of fairly simple equations. For rotation of

inner cylinder with zero axial flow the correlation proposed was

$$Nu = 0.409\left(\frac{T_a^2}{F_g}\right)^{0.241} - 137\left(\frac{T_a^2}{F_g}\right)^{-3/4} \quad 1700 < \left(\frac{T_a^2}{F_g}\right) < 10^7 \quad \ldots (2.04)$$

where,

$$F_g = \text{geometrical factor} = \left(\frac{\pi^4}{1697}\right)\left(1 - \frac{D}{2r_m}\right)^{-2} P^{-1}$$

and

$$P = 0.057\left[1 - 0.652\left(\frac{D/r_m}{1 - \frac{D}{2r_m}}\right)\right] + 0.00056\left[1 - 0.652\left(\frac{D/r_m}{1 - \frac{D}{2r_m}}\right)\right]^{-1}$$

They did not propose any correlation for combined axial flow with rotation. The data was taken for air. The heating element was wound helically around the inner cylinder.

Ho, Nardacci and Nissan's(9) analytical solution for the heat transfer characteristics of the Taylor Vortex system were restricted to systems with Prandtl number close to unity, narrow gap geometry and small temperature differences between inner and outer cylinder surfaces. System was electrically heated. The data was obtained for air. The correlation obtained was

$$Nu = 2\left[1 + 1.4472\left(1 - \frac{1700}{T_a^2}\right)\right] \quad \text{for } Pr \text{ close to } 1 \quad \ldots (2.05)$$

Singh and Ghosh(4) also studied heat transfer in concentric pipe heat exchanger with inner pipe rotating. Their work deals with the effect of inner pipe rotation on

annulus heat transfer in a double pipe heat exchanger. A quantitative measurement of heat transfer rate for the fluid flowing through the annulus and steam through the inner pipe was done in their investigation. The data were correlated in form of dimensionless groups. Water, undiluted molasses and four different dilutions of molasses-water were used. Following correlations were found for different ranges of Re and Pr.

$$(Nu)_T = (Nu)_a + (Nu)_r \qquad \ldots (2.06)$$

$$(Nu)_a = 0.55(Re)^{0.455}(Pr)^{1/3}\left(\frac{\mu_a}{\mu_w}\right)^{0.14} \quad 10 < Re < 2100,\ 4.5 < Pr < 600 \qquad \ldots (2.07)$$

$$(Nu)_a = 0.90(Re)^{0.9}(Pr)^{1/3}\left(\frac{\mu_a}{\mu_w}\right)^{0.14} \quad 5 < Re < 90,\ 900 < Re < 2900 \qquad \ldots (2.08)$$

$$(Nu)_a = 0.018(Re)^{0.895}(Pr)^{1/3}\left(\frac{\mu_a}{\mu_w}\right)^{0.14} \quad 2200 < Re < 4500,\ 4.5 < Pr < 600 \qquad \ldots (2.09)$$

$$(Nu)_r = 6.55\times10^{-9}(Re)^{1.675}(Pr)^{2.08}(N_{Ta})^{0.65} \qquad \ldots (2.10)$$

The increase in heat transfer was found to be 120 percent compared to the case of inner pipe at rest.

2.42 The beneficial effects of swirling motion produced by twisted strips were recognised by Reyes(5) as early as 1921. These effects have since been examined by various investigators such as Kirov, Nagesha and Bhogal(5). However,

these published results covered only a small range of test variables and were limited to specific test configurations, so that no generalized correlation predictions were possible. Margolis(5), Smith(5) and Koch(5) presented data in sufficient detail to permit further evaluation of the test results. Koch showed 110 percent increase in heat transfer for air. Margolis and Smith reported data for air and water.

Cambill et al.(5) presented data and empirical correlations for convective and boiling axial flows with water in electrically heated tubes. Due to the large experimental scatter encountered by these authors no definite conclusion was drawn on the friction effects. The heat transfer data obtained were more consistent.

Crocewell(5) performed tests concerned with the basic fluid flow phenomenon in a twisted strip assembly. He also attempted to fit empirical correlations to the friction data of Margolis.

Smithberg and Landis(5) studied velocity distribution, friction losses and heat-transfer characteristics analytically and experimentally for fully developed turbulent flow in tubes with twisted tape axial generators. Data were obtained for pitch to diameter ratios from 3.62 to 22.0 with both air and water under isothermal and forced convection heating conditions. They also predicted approximate heat

transfer correlations from Colburn-type analysis. The correlation predicted is

$$Nu = \frac{(1 + \frac{2}{\pi}\eta_0) Re\ Pr}{1 + \frac{700}{Re_s}(\frac{p}{H})(\frac{D_H}{D})Pr^{0.752}} \left[\frac{50.9(\frac{f}{2})}{Re\sqrt{2}} + .023(\frac{D}{D_H})Re^{-0.2}Pr^{-2/3} \times (1 + \frac{0.0219}{(\frac{H}{D})^2 e})\right] \quad \ldots (2.11)$$

where, η_0 = overall fin effectiveness of twisted strip,

H = helical pitch,

D_H = hydraulic diameter,

The increase in heat-transfer coefficient for air was found to be 125 percent compared to heat transfer coefficient in axial flow.

Rao and Date(6) investigated the performance of twisted steel strips of different pitch to diameter ratios as swirl generators in forced convection heat transfer. The test section was electrically heated and fluid used was water. The heat transfer coefficient was found to be a function of pitch and Reynolds number, and its value increased with the increase in the number of twists upto a particular value. A dimensionless correlation was proposed by them

$$0.270\ at\ Re_D^{0.63} = 149.4(\frac{H}{D}) - (\frac{12.4}{H/D})^2 + (\frac{88.27}{H/D})^3 \quad 0.5 \times 10^3 < Re_D (H/D = \infty) < 1.4 \times 10^5$$
$$7 \leq H/D \leq \infty \quad \ldots (2.12)$$

thore.

Re_D is Reynolds number.

H is pitch of helix.

D is the diameter of tube.

2.43 Boelter and Perlmutter(7) made an analysis of the velocity, temperature and pressure distributions in a turbulent vortex with radial and axial flow. The fluid was entering the inner tube tangentially. Tangential velocity, temperature and pressure distributions, as well as curves for overall energy or temperature separation, were presented and compared with experiment. No correlation was proposed by them.

Sherm et al(8) made observations on the overall heat transfer coefficient in horizontal double pipe heat exchanger with a swirl chamber attached using water, and steam as heating medium. They reported an increase in the overall heat-transfer coefficient substantially at a nominal power expense in creating the swirling flow. They did not attempt to correlate their data.

The critical appraisal of the literature review reveals that apparently no information is available regarding the heat transfer to swirling flow produced by tangential inlets. The probable reason could be that the flow reversal proved detrimental to heat-transfer operations, but now since it has been possible in our laboratory

to produce such swirling flow in long tubes without the reversal of axial component, it is proposed to predict and test the model for heat transfer for this system.

CHAPTER - 3

EXPERIMENTAL METHOD FOR PRESSURE DROP AND HEAT TRANSFER COEFFICIENT

3.00 Equipment for study of heat transfer to swirling flow in long tube was fabricated as per sketch shown in Fig. 3.01. It consists of a swirl chamber machined from 25 mm thick perspex plate. The plates were held together by four 6 mm dia rods. To this swirl chamber, inside tube of the double pipe heat exchanger was fixed by stuffing box arrangement. Individual plates of the swirl chamber were provided with a set of two tangential inlet nozzle placed diametrically opposite to each other.

3.10 PRESSURE DROP

Analytical Prediction

The overall pressure drop between tangential inlet and outlet, recorded by a pressure gauge shall include:

(i) The loss due to sudden expansion of cross-section,

(ii) The loss due to sudden contraction of cross-section,

(iii) Radial pressure drop at the entry head,

(iv) Pressure drop due to friction in swirl flow, and

(v) Pressure drop due to friction in tangential entry pipes.

0

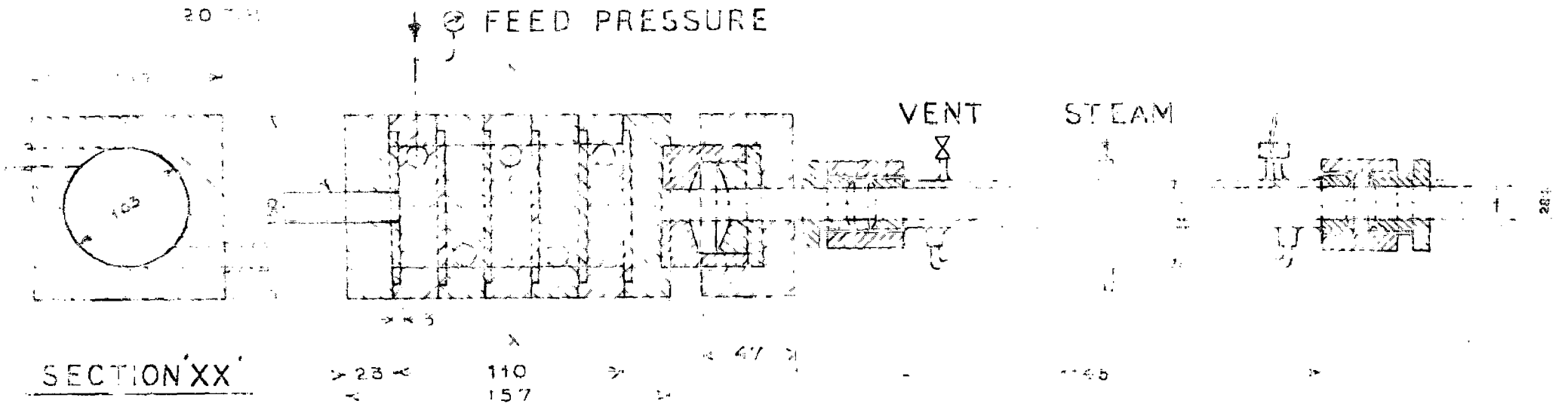

FIG. 3.01 DETAILS OF SWIRL FLOW HEAT EXCHANGER
ALL DIMENSIONS IN mm

Total pressure drop thus observed experimentally will be equal to the sum of all the pressure drops mentioned above.

$$\Delta P = (\Delta P_1 + \Delta P_2 + \Delta P_3 + \Delta P_4 + \Delta P_5) \qquad \ldots (3.01)$$

The various pressure drops are as detailed below:

3.11 PRESSURE DROP DUE TO SUDDEN EXPANSION OF FLOW DIRECTION (25)

When the liquid enters the swirl chamber through tangential entry, the area-section of the pipe is suddenly enlarged, the fluid stream separates from the wall and issues as a jet into the enlarged section. The jet then expands to fill the entire area-section of the swirl chamber. The space between the expanding jet and the swirl chamber wall is filled with fluid in vortex motion and considerable turbulence is generated within this space. If the velocities at two area-sections are known then,

$$\frac{\Delta P_1}{\rho} = \frac{(V_1 - V_2)^2}{2g_0} \qquad \ldots (3.02)$$

3.12 PRESSURE DROP DUE TO SUDDEN CONTRACTION OF FLOW DIRECTION (25)

When the liquid flows to the pipe through swirl chamber, the cross section of the pipe is suddenly reduced, the fluid stream cannot follow around the sharp corner, and the stream breaks contact with the wall of the pipe.

A jet is formed, which flows into the stagnant fluid in the smaller section. The jet first contracts and then expands to fill the smaller cross-section, and downstream from the point of contraction the normal velocity distribution eventually is re-established.

The loss from sudden contraction is proportional to the velocity head in the smaller pipe and can be calculated by the equation,

$$\frac{\Delta P_2}{\rho} = K_c \frac{V_b^2}{2G_c} \qquad \ldots (3.03)$$

where the proportionality factor K_c is called the contraction-loss coefficient and V_b is the average velocity in the smaller or downstream section.

3.13 RADIAL PRESSURE DROP AT THE INLET END

The radial pressure drop can be computed by

$$\frac{\Delta P_1}{\rho} = \frac{v^2}{2G_c}\left[\frac{1}{r^2} - \frac{1}{R^2}\right] \qquad \ldots (3.04)$$

which may be derived using Navier Stokes equation (7).

3.14 RADIAL PRESSURE DROP DUE TO FRICTION IN SMALL PIPE

$$\frac{\Delta P_f}{\rho} = \frac{4f\, L_c V_c^2}{2G_c D_H} \qquad \ldots (3.05)$$

Darcy friction factor 'f' may be computed from

$f = .0791/(R)^{0.25}$ for $2.1 \times 10^3 < R < 10^5$ ... (3.06)

3.15 PRESSURE DROP DUE TO FRICTION IN THE ANNULAR ENTRY PORTS

Some pressure drop may be expected in the approach pipes to the entry head. Though the pressure drop will be quite small it may be computed using the equation (3.05).

In the analytical prediction of heat transfer only the radial pressure drop at entry head equation (3.04) and pressure drop due to friction in axial flow equation (3.05) will be used. All other pressure drops are not needed as they do not help in the heat transfer in test-section. So the total pressure drop for this purpose shall be

$$(\Delta P)_T = \Delta P_3 + \Delta P_4 \qquad \ldots (3.06)$$

3.2 FLUID FRICTION-ANALYTICAL PREDICTION

In order to predict friction losses in the axial flow heat exchanger a model of the boundary layer must be formulated.

The actual boundary layer will reflect the influence of both the axial and the tangential velocity components. It should be expected that the sublayer will be thinner than in pure axial flow due to the superposed vortex motion. Unfortunately, there exists no information on axial boundary layer of this type and the simplifying

assumptions made in the subsequent analysis can be rationalised only in the absence of better information.

The proposed boundary layer model assumes that both the axial and the tangential velocity components can be expressed as functions of y/δ, where for the axial component the usual specifications for the laminar sub-layer and the buffer zone,

$$u^+ = y^+ \qquad 0 \leqslant y^+ \leqslant 5 \qquad \ldots (3.07a)$$

$$u^+ = -3.05+3.0 \ln y^+ \qquad 5 < y^+ \leqslant 30 \qquad \ldots (3.07b)$$

are applicable.

The tangential component is taken to vary linearly across this portion of the boundary layer and is given by

$$V_\theta = V_\theta\left(\frac{V_a}{V_a}\right) \qquad 0 \leqslant y^+ \leqslant 30 \qquad \ldots (3.08)$$

which follows from the free vortex relationship $V_0 = \Omega/r$, where Ω is known as circulation constant. In free vortex motion, the angular momentum i.e. the product of the tangential velocity component at any point and radius at any point in the liquid is constant i.e. $V'R = \Omega$. As V' is not easily amenable to evaluation, V_a has been substituted in place of V', where a represents the ratio of inlet velocity to the velocity attained at the metal wall.

If it is further assumed that the flow is essentially

incompressible, the mechanical energy losses due to the axial flow and the tangential flow may be added in the form of equivalent $\Delta P/\rho$ terms to define the overall friction factor

$$f = \left(\frac{\Delta P}{\rho}\right)_T \frac{C_o r_H}{2L_o V_o^2} \qquad \ldots (3.09)$$

From equation (3.06)

$$\left(\frac{\Delta P}{\rho}\right)_T = \frac{\Delta P_3}{\rho} + \frac{\Delta P_4}{\rho}$$

3.3 HEAT TRANSFER-ANALYTICAL PREDICTION

The physical model used in the friction analysis should also serve as a basis for the heat transfer predictions. The total transfer should therefore be due to the tube wall boundary layer flow.

As in any friction heat transfer correlation, the complexity of the results is a function of the boundary layer details and of the Prandtl number effects considered. To evaluate the heat transfer due to the axial and tangential tube wall flow, a modified friction factor f' will have to be defined. Using the concept of a modified Reynolds' analogy, all the shear effects along the tube wall should contribute to heat transfer. However only a portion of the tangential momentum transfer will have a convective counterpart since the dissipation caused by the 90^0 turn of the boundary fluid is not likely to contribute to heat transfer. Assuming that an

effective shear stress $\tau_{a,t}$ can be defined which is dependent on the total velocity vector at the edge of the laminar sub-layer,

$$\frac{\tau_{a,t}}{\tau_a} = \left(\frac{V}{u}\right)_{y^+=5} \qquad \ldots (3.10)$$

the heat transfer should increase in the same proportion. The equivalent friction factor f' for this part of the total heat transfer now becomes

$$f' = f_a\left(\frac{V}{u}\right)_{y^+=5} = 0.046\ Re^{-0.2}\left(\frac{V}{u}\right)_{y^+=5} \qquad \ldots (3.11)$$

where, $f_a = 0.046\ Re^{-0.2}$. Substituting $\delta = 30\nu/\bar{u}\sqrt{f/2}$ in (3.07a) and (3.08) and further substituting

$$(u)_{y^+=5} = 5\,\bar{u}\sqrt{\frac{f}{2}} \quad \text{and} \quad (V_0)_{y^+=5} = \frac{5}{30}\,\frac{V_1 cr_0}{r_w}$$

from the assumed sublayer velocity distribution, yields

$$f' = 0.046\left[1 + \frac{(V_1 cr_0/r_w)^2}{450\,\bar{u}^2 f}\right]^{1/2} Re^{-0.2} \qquad \ldots (3.12)$$

The Colburn analogy, which is based on $(T_w - T_b)$, leads to

$$q_{a,t} = \frac{f'}{2}\,\rho\bar{u}\,C_p Pr^{-2/3}(T_w - T_b) \qquad \ldots (3.13)$$

$$= 0.023\,\rho\bar{u}C_p Pr^{-2/3}\,Re^{-0.2}\left[1 + \frac{(V_1 cr_0/r_w)^2}{450\,\bar{u}^2 f}\right]^{1/2}(T_w - T_b) \qquad \ldots (3.13a)$$

Here $q_{a,t} = q_w$ $\qquad \ldots (3.14)$

and introducing the Stanton number,

$$\alpha = \frac{q_w}{\rho_D u(i_w - i_B)}, \text{ yields}$$

$$\alpha = C_0 C_3 Pr^{-2/3} Re^{-0.2}\left[1 + \frac{(v_1 \sigma r_0/r_w)^2}{450\ \bar{u}^2}\right]^{1/2} \quad \ldots (3.15)$$

This equation may also be expressed in terms of a dimensional Nusselt number,

$$Nu = \alpha\ Re Pr \left(\frac{D}{D_H}\right) \quad \text{or}$$

$$Nu = 0.023(Re)^{0.8}(Pr)^{1/3}\left[1 + \frac{(V_1(\sigma r_0/r_w)^2}{450 r_w^2\ \bar{u}^2}\right]^{1/2}\left(\frac{D}{D_H}\right) \quad \ldots (3.15a)$$

This method is based on bulk properties and should be modified by isothermal correction factor of $(\mu_w/\mu_B)^{-0.36}$ recommended by Deissler(11).

The final form of equation (3.15a) will therefore be

$$Nu = .023(Re)^{0.8}(Pr)^{1/3}\left[1 + \frac{(V_1 \sigma r_0/r_w)^2}{450 \bar{u}^2}\right]^{1/2}\left(\frac{D}{D_H}\right)\left(\frac{\mu_B}{\mu_w}\right)^{0.36} \quad \ldots (3.15b)$$

CHAPTER -4

EXPERIMENTAL INVESTIGATION

4.1 EXPERIMENTAL SET UP

To check the validity of the proposed model an experimental set up for obtaining data on heat transfer to swirling flow of liquids was set up. shown schematically in fig.4.01 and also presented in plate 4.01. It consisted of a double pipe heat exchanger in which the inner tube(1) was made of stainless steel having O.D = 31.8 mm. and I.D = 28.4 mm. A length of 1145 mm. of this tube was steam jacketed by using one and a half inch steam pipe (2) along with other necessary steam fittings. To one end of the inner tube of double pipe heat exchanger a swirl chamber(3) machined out of perspex was fixed by stuffing box arrangements. Inside diameter of the swirl chamber was 105 mm. Fig.3.01 shows details of a typical swirl chamber. Eight tangential inlets each of 1/2", 3/8", 2/8" and 1/8" inside diameter were symmetrically fixed to the swirl chamber. An axial inlet of one inch diameter (5) was provided for comparative studies in linear flow of liquid. Liquid was pumped by a 3 H.P. pump(6) to swirl chamber(3). A by-pass valve(16) and control valves (17,18,19) were used to control the flow through inner tube. Inlet pressures were recorded using calibrated pressure

of the liquid entering the test section was noted. The inlet and outlet temperatures of the liquid were noted. The pressure of the steam and also its temperature were recorded. The temperature of the condensate was also measured to check subcooling. The rate of the liquid was measured by weighing the liquid collected at the outlet over a known time interval. Data were obtained under steady state conditions. The liquids used in the investigation were water and three different dilutions of glycerine. The steam pressure was varied from 1.4 to 2.2 kg/cm^2.

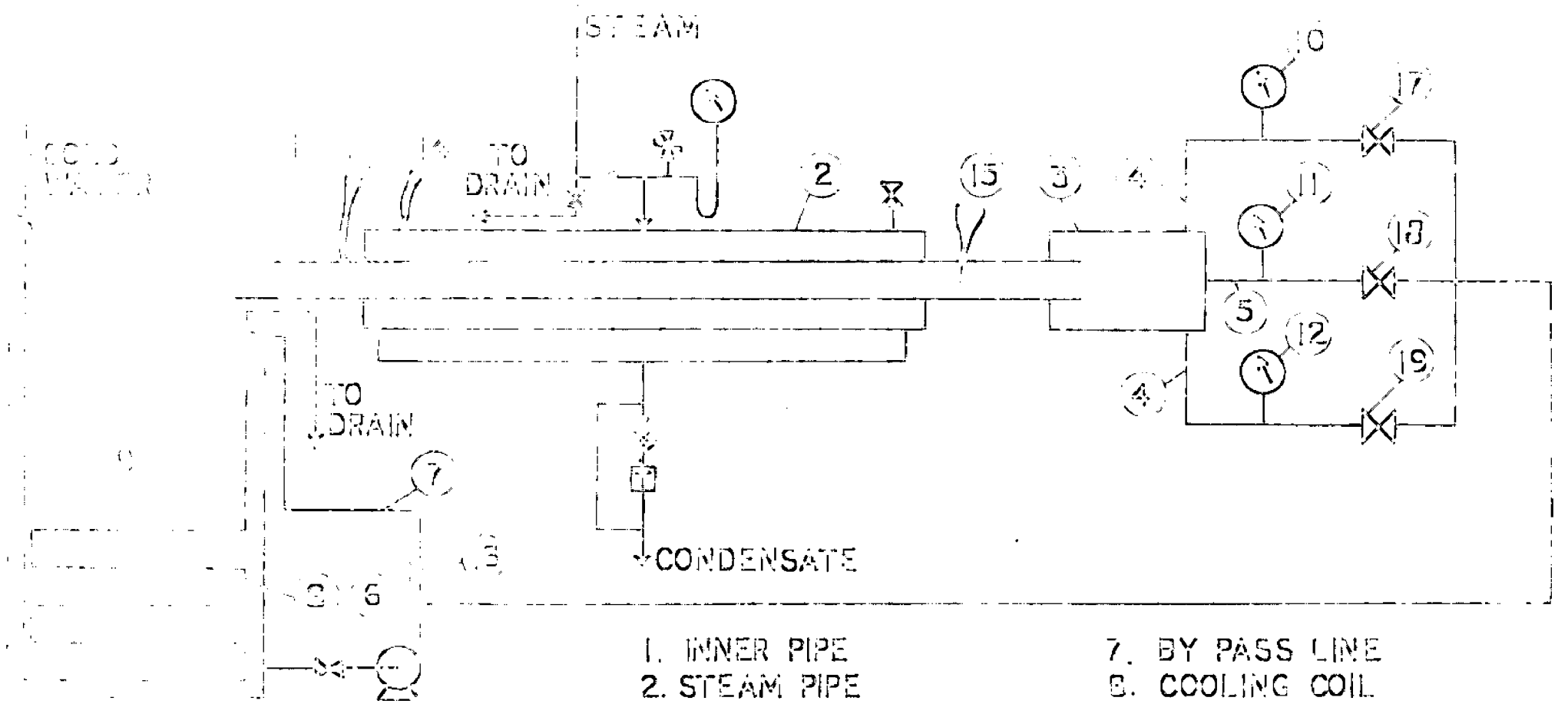

1. INNER PIPE
2. STEAM PIPE
3. SWIRL CHAMBER
4. TANGENTIAL INLET
5. AXIAL INLET
6. PUMP
7. BY PASS LINE
8. COOLING COIL
9. FEED TANK
10,11,12. PRESSURE GAUGES
13,14,15. THERMOCOUPLES
16. BY PASS VALVE

SCHEMATIC DIAGRAM OF EXPERIMENTAL SETUP

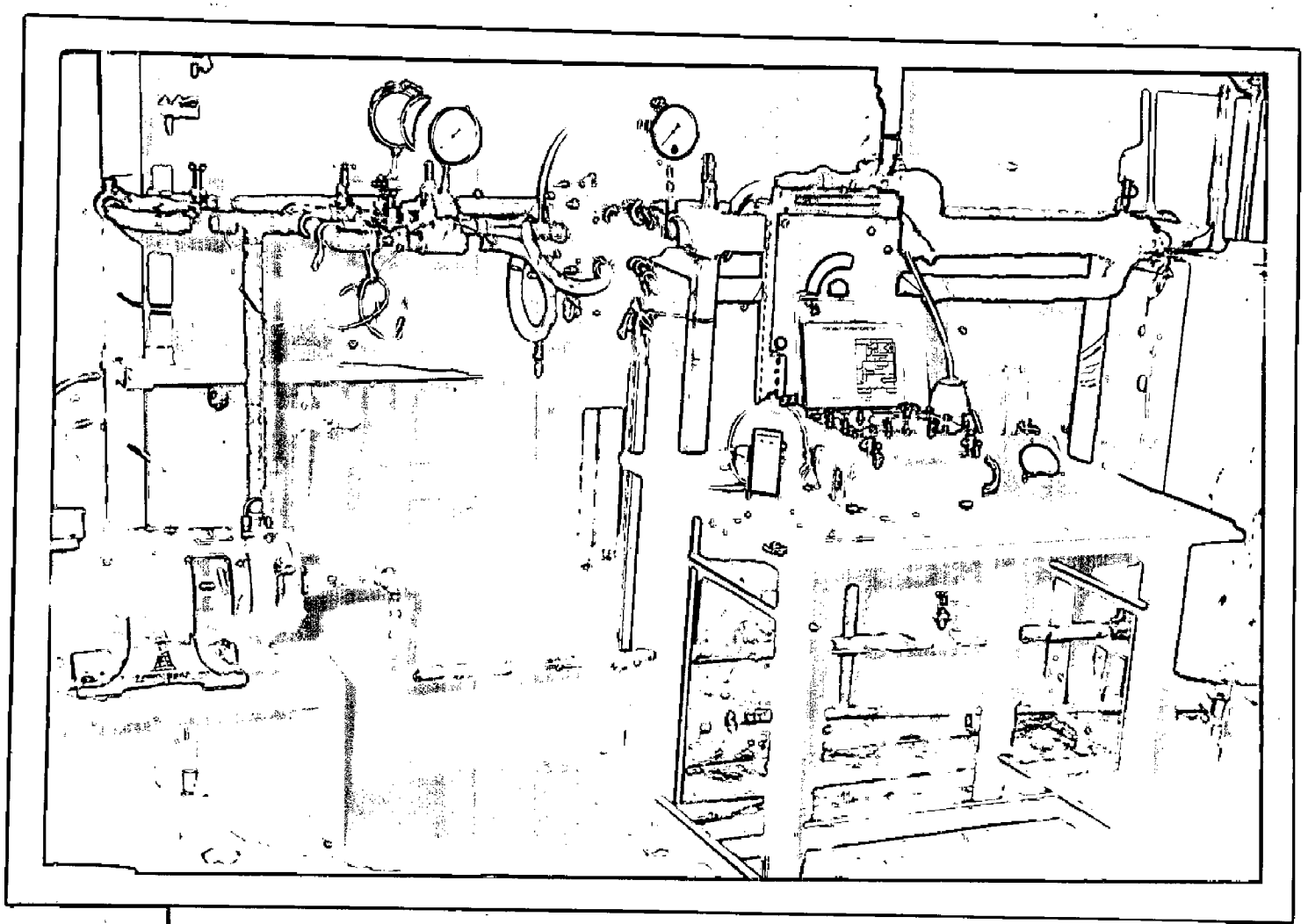

PLATE 4.01 OVERALL LAYOUT OF APPARATUS

gauges (10,11,12). Liquid was received in feed tank(9) fitted with a cooling coil(8). Cold water was passed through the cooling coil. Liquid was recirculated to the heat exchanger after cooling in the tank. The heat exchanger was lagged with asbestos rope and plastered with plaster of Paris to reduce the heat losses. The entire assembly was supported on a mild steel stand.

The inlet and outlet temperatures of the liquid and steam temperatures were measured by means of calibrated copper-constantan thermocouples (13,14,15). All the thermocouples were connected through cold junctions to a D.C. potentiometer. The cold junction was kept in a melting ice bath to obtain a reference temperature of 0°C. The e.m.f. of thermocouples was measured by a D.C. potentiometer. The measurements were made upto 0.01 m.v. with an accuracy of 0.01 percent.

4.2 EXPERIMENTAL PROCEDURE

The thermocouples were calibrated against a standard mercury in glass thermometer of 0.1°C least count. The average reading of the thermocouple was 0.6° less than the actual reading of the thermometer.

The pump supplied the process liquid from the tank to the test section through the swirl flow. The pressure

CHAPTER 5

EXPERIMENTAL RESULTS AND DISCUSSION

To test the validity of the model it was decided to confirm the effect of variation of tangential inlet velocity, tangential inlet diameters, and kinematic viscosity of the fluid at different steam temperatures.

5.10 EFFECT OF TANGENTIAL INLET VELOCITY

Effect of variation of tangential inlet velocity on heat-transfer coefficient is given in Tables 5.01 to 5.07, and Figs. 5.01 and 5.02 depict the effect of tangential inlet velocity on liquid side film coefficient. It can be safely concluded that the liquid film coefficient increases with tangential inlet velocity. Figs. 5.03 and 5.04 depict the comparison of liquid side film coefficient calculated from the model with the experimental results. It can be concluded from the figures that about 90 percent of the data falls within ± 25 percent.

5.11 EFFECT OF TANGENTIAL INLET DIAMETER

Tables 5.01 to 5.04 and Fig. 5.01 show the effect of variation in tangential inlet diameters on the liquid side film coefficient. It is observed from the figure (5.01) that with the decrease in the size of tangential entry the liquid

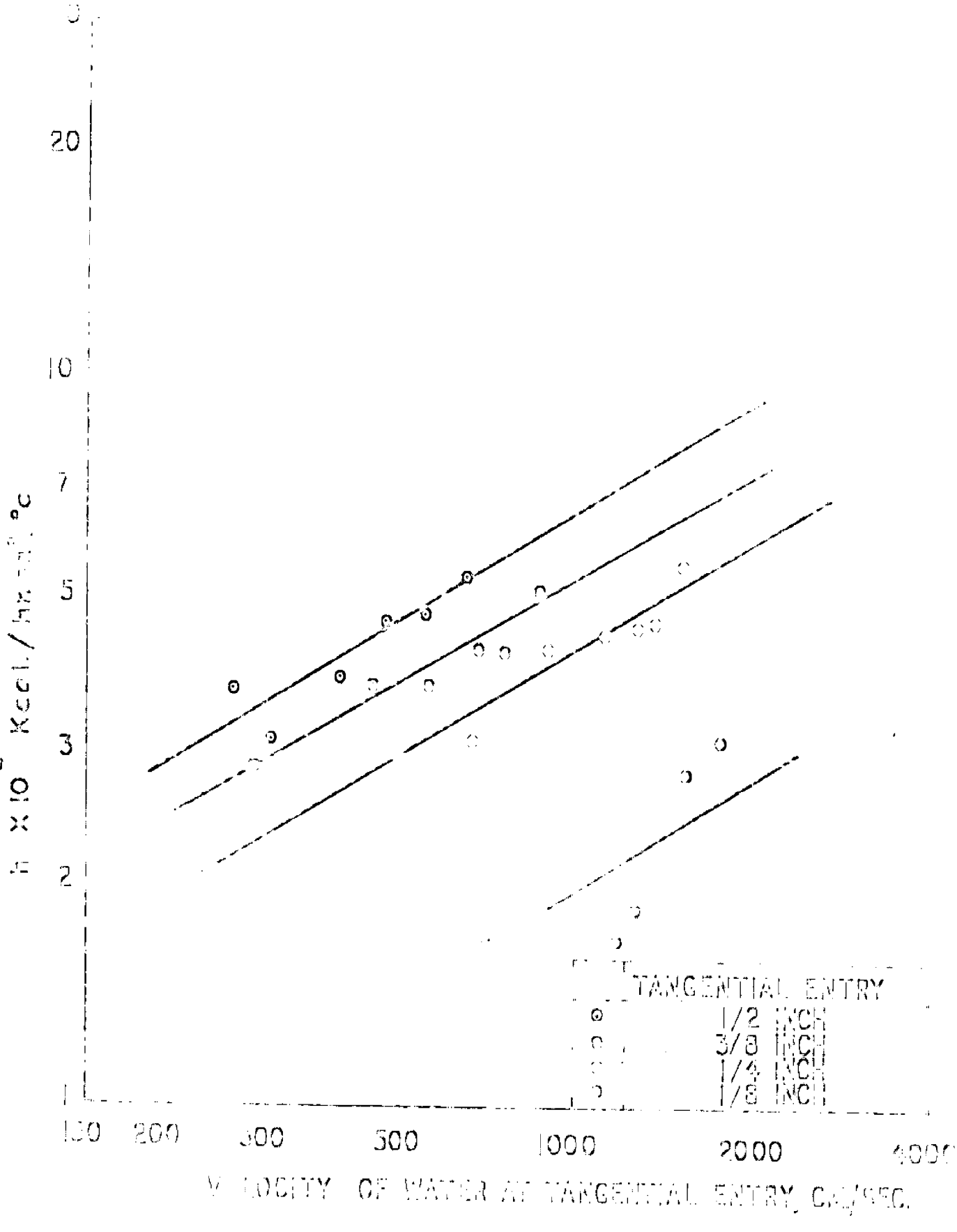

VARIATION OF HEAT TRANSFER COEFFICIENT WITH VELOCITY AND TANGENTIAL ENTRY FOR WATER

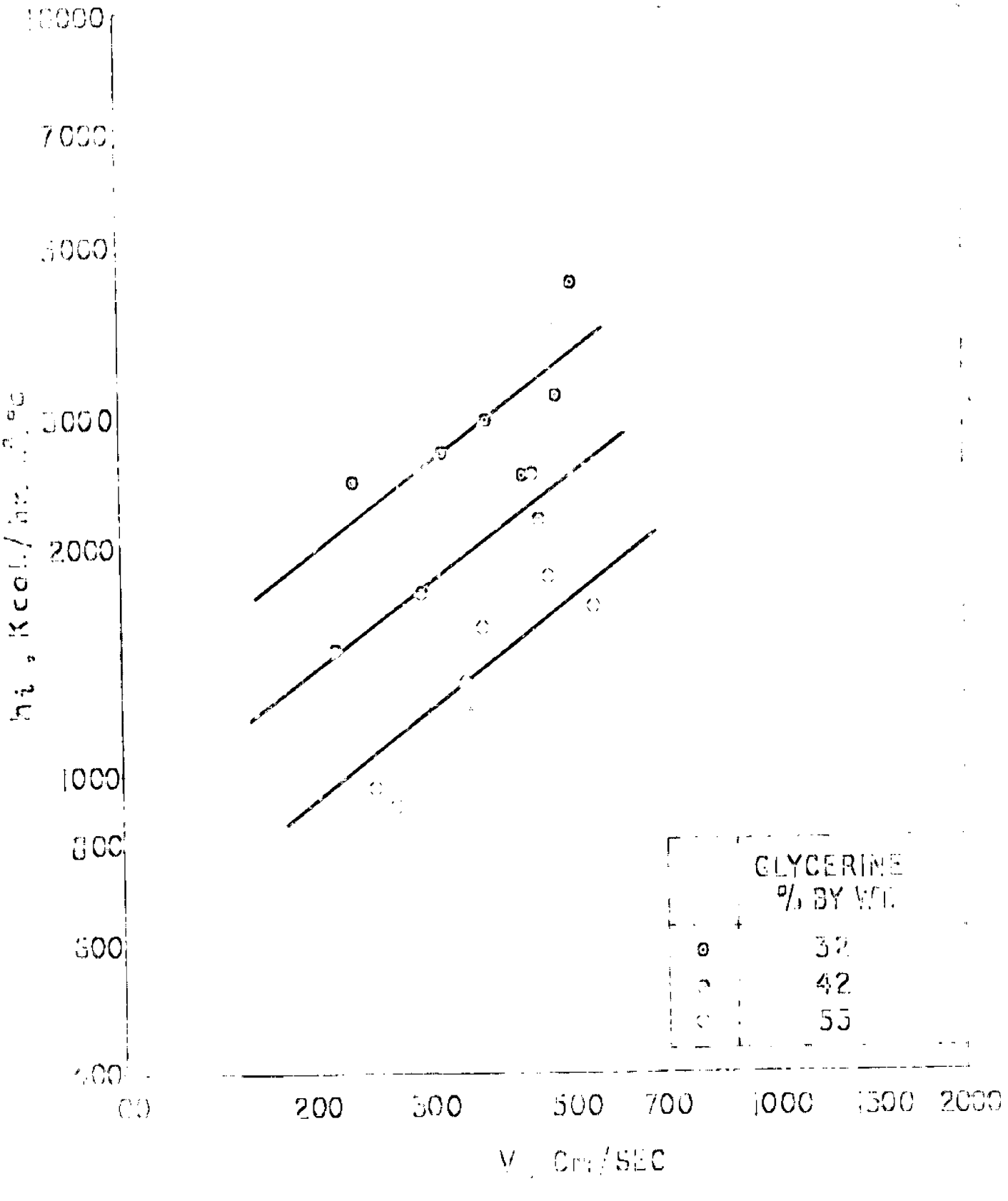

VARIATION OF HEAT TRANSFER COEFFICIENT WITH VELOCITY AT TANGENTIAL ENTRY AND VISCOSITY FOR GLYCERINE

film heat transfer coefficient decreases. To show this effect four tangential entries of diameters 1/2", 3/8", 1/4" and 1/8" are used.

5.12 EFFECT OF VISCOSITY

To study the effect of viscosity on liquid side film coefficient three glycerine-water mixtures of different concentrations were used. Table 5.03 to 5.07 and fig. 5.02 show the effect of variation of viscosity on liquid side film coefficient. It is observed from the Fig.5.02 that as the viscosity of the liquid increases, the liquid film coefficient decreases.

5.13 EFFECT OF STEAM TEMPERATURES

Effect of variation in steam temperature on liquid side film coefficient is shown in figure 5.05. The data was taken on different steam temperatures to study this effect. It is concluded from the Fig.5.05 that the variation in steam temperature does not affect the liquid film coefficient directly.

The heat transfer data for axial flow is also taken for the comparison purposes. Table 5.08 and Fig.5.06 show the effect of variation in the mass flow rate on the heat-transfer coefficient for axial flow.

Data for RUN of swirl for different flow rates through the tube with different tangential entries are taken from Sharma(12). These data are given in table 5.09.

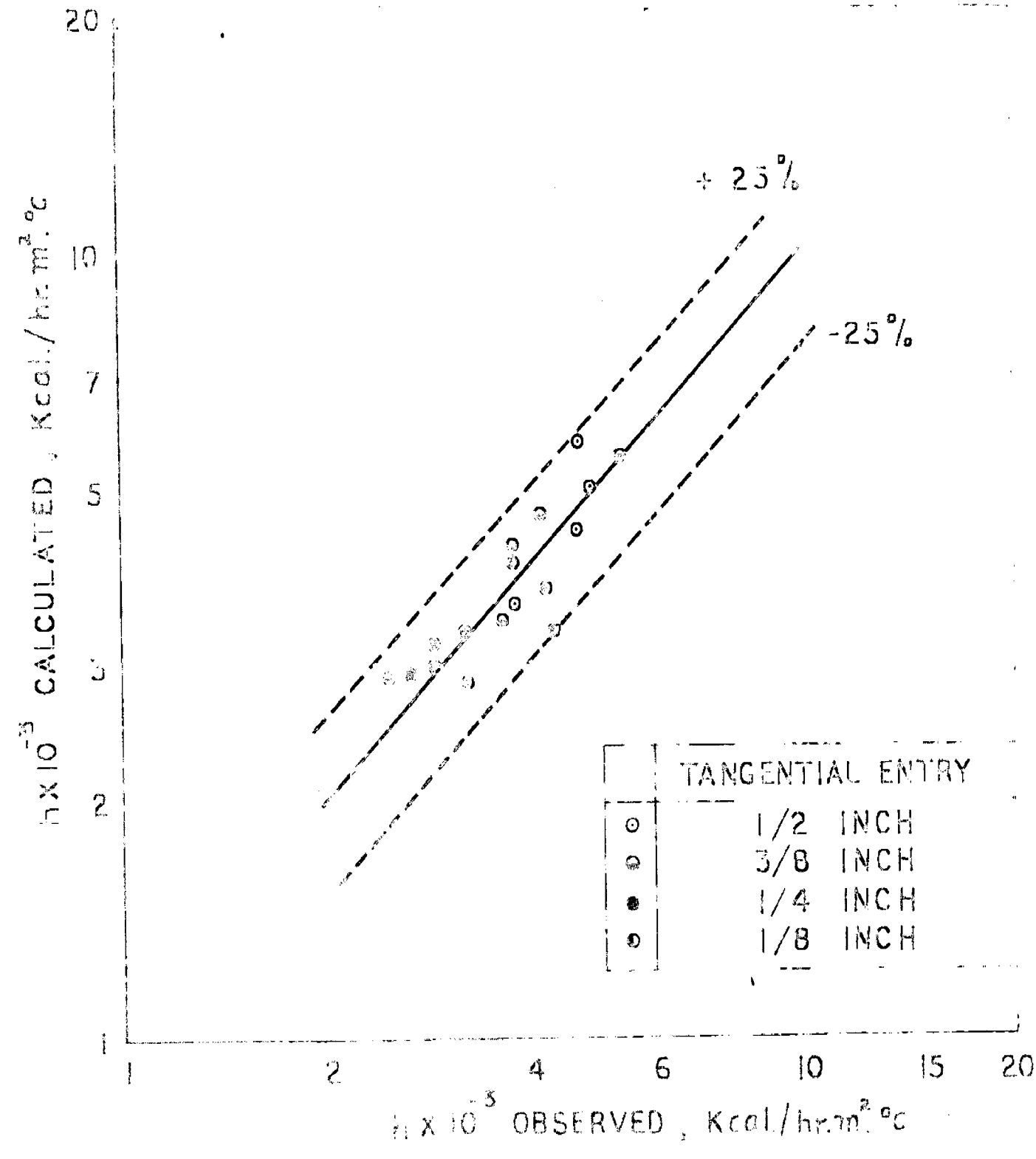

FIG.5.03 VARIATION OF HEAT TRANSFER COEFFICIENT OBSERVED AND CALCULATED FOR WATER FROM CORRELATION EQUATION 3.15 b

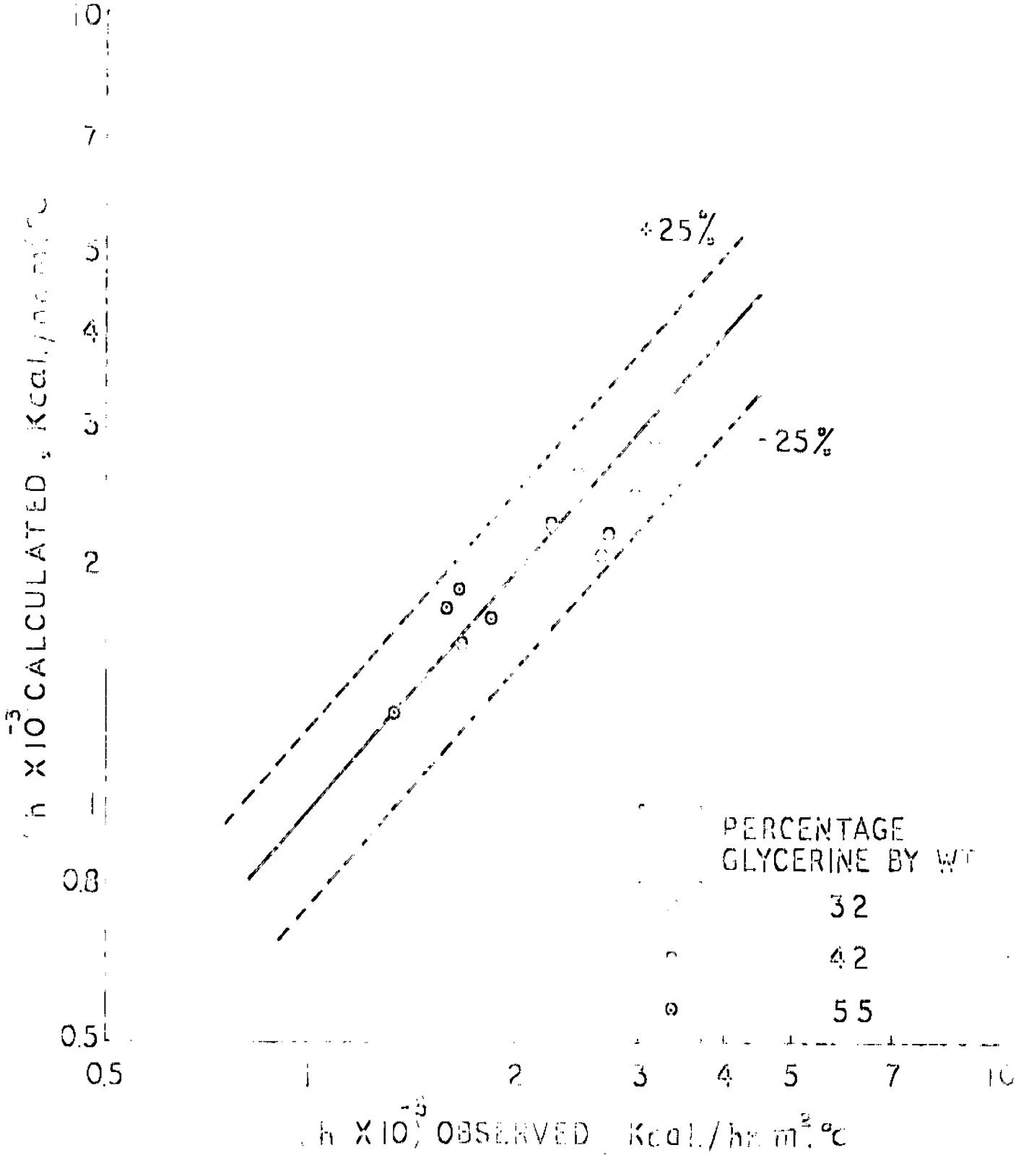

FIG. VARIATION OF HEAT TRANSFER COEFFICIENT OBSERVED AND CALCULATED FOR GLYCERINE FROM CORRELATION EQUATION 3.15 b

Steam coefficients for different data are obtained from Wilson's plot.

5.2 DISCUSSION

In a long tube it is possible to have a much higher velocity of liquid at any point on heat transfer surface in a swirling flow as compared to the velocity of the axial flow for the same throughput and the rotation in the liquid creates additional turbulence which in turn helps to enhance the rate of heat transfer in the heat exchanger. The centrifugal acceleration produced by free vortex type of swirling flow gives rise to a high buoyant force to liquid in contact with the hot surface of the tube as soon as it loses in density because of temperature rise. Thus a uniform temperature will be developed in the layer of the liquid to which the heat is being transferred. This increases the liquid film coefficient inside the tube and improves the performance of the heat exchanger. The liquid side film coefficient for water increases by 110 percent for 1/2 inch tangential entry, by 140 percent for 3/8 inch tangential entry, by 185 percent for 1/4 inch tangential entry, by 240 percent for 1/8 inch tangential entry for the same flow rate as compared to axial flow. The comparison is shown in Fig.5.06.

It has been observed that in this system, the liquid

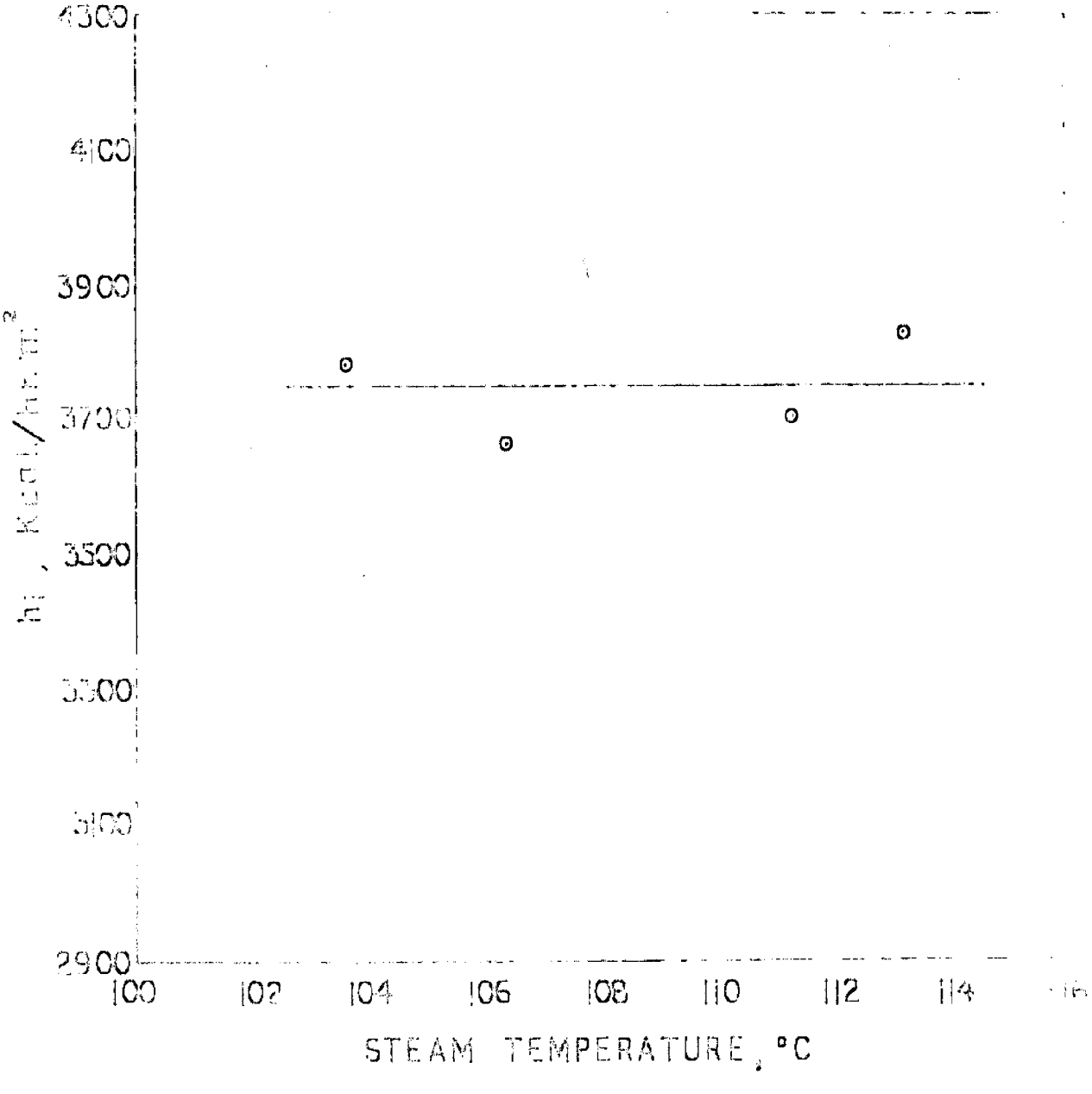

FIG. 5.0 5 VARIATION OF HEAT TRANSFER COEFFICIENT WITH STEAM TEMPERATURE

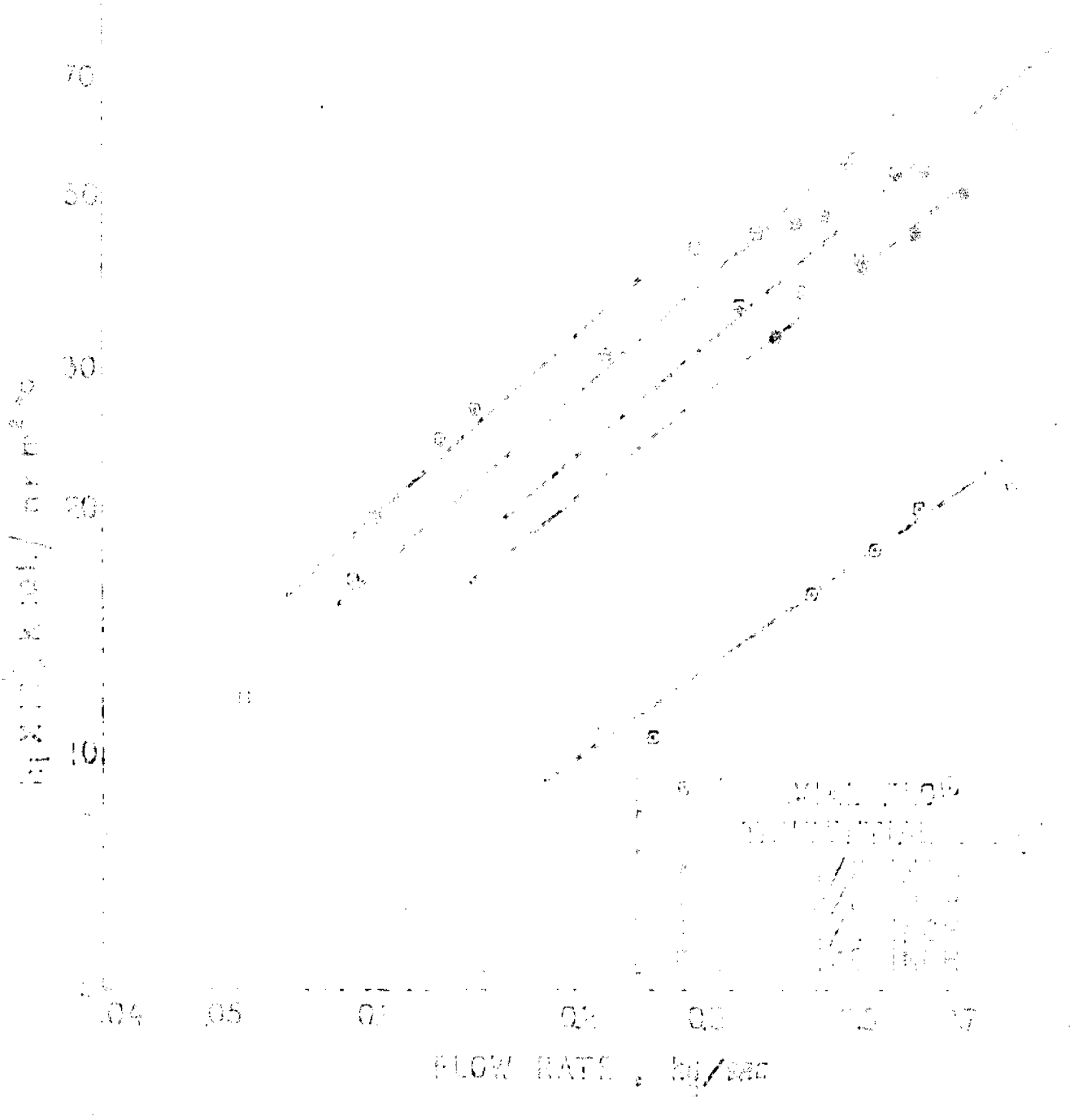

FIG. 5.0.6 VARIATION OF h_i WITH FLOW RATE

film coefficient is not the controlling factor but steam film is equally responsible for resistance to heat flow. Since the steam film coefficient is a function of heat flux, the increase in liquid film coefficient indirectly increases the steam side film coefficient also.

From computed values it is noted that 90 percent of the data lie within ±25% of the observed heat-transfer coefficient. Figures 5.03 and 5.04 are plots between heat-transfer coefficient observed and heat transfer coefficient calculated from the proposed model. The deviation in heat transfer calculated from the model and the observed heat transfer coefficient can be attributed to experimental error.

Table 5.01- Experimental data for Heat Transfer to water for 1/2" Tangential Entry

Steam condensing rate=5000 $\frac{KCal}{hr.m^2.°C}$

Run No.	Water Inlet Pressure Psig	Water Temp. °C Inlet	Water Temp. °C Outlet	Steam Temp. °C	Water flow Rate kgs/sec.	U $\frac{KCal}{hr.m^2.°C}$	h_i observed $\frac{KCal}{hr.m^2.°C}$	h_i Calculated KCal/hr.m²°C
1	1	97.95	50.20	103.65	0.3942	2510	5700	
2	2	96.15	47.00	103.65	0.3670	2500	5092	5582.4
3	3	95.40	44.60	103.65	0.5000	2190	5940	4491.0
4	4	99.40	43.20	103.65	0.6060	2200	5740	5090.0
5	5	95.20	42.10	102.00	0.7050	2100	5007	5709.5
6	6	94.90	41.20	102.00	0.8925	2750	5179	-
7	1	99.90	47.20	106.40	0.3942	2200	5660	-
8	2	99.50	46.10	106.40	0.3670	2200	5751	5574.0
9	3	99.90	44.70	106.40	0.5000	2060	4677	4402.0
10	4	95.20	44.90	106.40	0.6060	2070	4691	4947.0
11	5	95.40	43.20	106.40	0.7050	2004	4642	5699.0
12	6	99.69	41.09	106.40	0.8925	2500	4010	-
13	1	99.90	48.25	111.90	0.3942	2270	5700	-
14	2	99.90	45.65	111.90	0.3670	2070	5195	5651.0
15	3	99.60	44.90	110.66	0.5000	2520	5076	4517.5
16	4	94.20	44.03	110.66	0.6060	2903	4610	5102.0
17	5	94.20	42.60	110.66	0.7050	2600	4726	5768.4
18	6	94.70	42.50	110.66	0.8925	2700	5500	-
19								
20	1	94.90	48.70	119.19	0.3942	2300	5820	-
21	2	94.90	47.10	119.19	0.3670	2100	5910	5420.0
22	3	94.70	45.00	119.19	0.5000	2400	4090	5090.0
23	4	94.70	44.70	119.19	0.6060	2500	4620	4002.0
24	5	95.00	44.00	119.19	0.7050	2700	5070	4225.0
25	6	95.00	43.50	119.19	0.8925	2970.	6020	-

Table 5.02- Experimental data for Heat Transfer to water for S/C's Tangential Entry

Steam coefficient = 5560 $\frac{K Cal}{hr.m^2\ ^oC}$

Sr. No.	Water Inlet Pressure psig	Water Temp. °C Inlet	Water Temp. °C Outlet	Steam Temp. °C	Water flow rate K Cal kgs/sec	U $\frac{K Cal}{hr.m^2\ ^oC}$	h_i Observed $\frac{K Cal}{hr.m^2.^oC}$	h_i Calculated $\frac{K Cal}{hr.m^2.^oC}$
[illegible]	1	92.60	92.7	102.2	0.2014	8870	5560.0	-
	2	94.25	46.12	102.2	0.3305	8802	5600.0	5400.0
	3	93.50	44.50	102.2	0.4070	8850	5730.0	4228.0
	4	93.50	49.90	102.2	0.4950	8900	4100.0	4650.0
	5	95.00	40.50	102.2	0.5525	8791	5560.0	5515.0
	6	95.45	49.50	102.2	0.6200	8796	5575.0	-
[illegible]	1	93.80	94.90	100.9	0.2014	8905	2900.0	-
	2	95.00	49.60	100.9	0.3305	8800	5670.0	5000.0
	3	96.35	40.00	100.9	0.4070	8800	5070.0	4804.0
	4	93.00	48.05	100.9	0.4950	8900	4223.0	5465.0
	5	97.55	46.65	100.9	0.5525	8900	4223.0	5517.4
	6	98.75	47.00	100.9	0.6200	8890	5105.0	-
[illegible]	1	93.00	95.25	110.7	0.2014	8850	3250.0	-
	2	96.15	50.60	110.7	0.3305	8890	5724.0	5555.0
	3	97.10	40.05	110.7	0.4070	8890	4192.0	4004.0
	4	40.90	52.50	110.7	0.4950	8850	4642.5	6150.0
	5	96.15	46.40	110.7	0.5525	8890	4045.0	5407.0

Table 5.03 Experimental Data for Heat Transfer to water for 1/4 inch. Tangential entry

Steam coefficient = 5560 $\frac{\text{KCal}}{\text{hr.m}^2.^0\text{C}}$

Run No.	Water Inlet Pressure psig	Water Temp °C		Steam Temp °C	Water Flow rate kg/sec.	U KCal/hr.m^2 °C	h_i Observed KCal/hr. m^2 °C	h_i Calculated KCal/ hr.m^2.°C
		Inlet	Outlet					
1.	2	31.85	50.55	102.2	0.2122	2020	3197.4	2020
2.	4	32.2	48.50	102.2	0.2870	2550	4192.0	3700
3.	6	32.2	46.10	102.2	0.3530	2460	4420.0	
4.	8	32.57	45.90	102.2	0.4040	2690	5220.0	
5.	10	33.05	44.70	102.2	0.4400	2620	4770.0	
6.	12	33.05	44.25	102.2	0.4800	2695	5225.0	
7.	2	32.34	51.50	108.2	0.2122	1990	2069.4	2906
8.	4	33.5	50.60	107.3	0.2870	2950	4070.4	3650
9.	6	34.0	48.95	107.3	0.3530	2550	4650.0	
10.	8	34.22	47.53	107.3	0.4040	2590	4720	
11.	10	37.35	48.95	107.3	0.4400	2500	4675	
12.	12	36.97	47.8	107.3	0.4800	2700	5480	
13.	2	34.7	54.50	111.1	0.2122	2020	3140.1	2956
14.	4	35.4	52.7	111.1	0.2870	2488	4288.6	3240
15.	6	35.65	50.0	111.1	0.3530	2400	4475	
16.	8	36.37	49.07	111.1	0.4040	2580	4575	
17.	10	36.37	48.95	111.1	0.4400	2594	4650	
18.	12	36.37	48.25	111.1	0.4800	2750	5450	
19.	2	34.7	56.30	115.3	0.2122	2100	3755.4	4020
20.	4	35.65	53.05	115.3	0.2870	2280	5375	2850
21.	6	36.15	52.24	115.3	0.3530	2580	4615	
22.	8	38.3	52.50	115.3	0.4040	2970	4700	
23.	10	40.7	54.10	115.3	0.4400	2700	5400	
24.	12	38.05	50.02	115.3	0.4800	2750	5450	

Table 5.04 Experimental data for Heat Transfer to Water for 3/C" Horizontal Entry.

Steam Coefficient= 5000 $\frac{KCal}{hr.m^2.^oC}$

Run No.	Water Inlet Pressure psig	Water Temp. °C Inlet	Water Temp. °C Outlet	Steam Temp. °C	Water Flow Rate kg/cm.	U $\frac{KCal}{hr.m^2.^oC}$	h_i Observed $\frac{KCal}{hr.m^2.^oC}$	h_i Calculated $\frac{KCal}{hr.m^2.^oC}$
1	3	31.00	54.75	98.15	.06575	670	1092	
2	6	29.90	51.05	201.55	.0952	1027	1290	
3	9	31.15	57.75	202.69	.09975	1760	2256	
4	12	30.90	57.05	202.05	.1250	1745	2401.5	2770
5	15	31.60	56.00	202.65	.1591	1910	2029	2145.9
6	3	31.15	54.75	200.2	.06575	901	1100	
7	6	31.05	51.05	200.2	.09920	1350	1750	
8	9	33.05	57.75	200.2	.09975	1475	1970	
9	12	33.05	57.05	207.05	.12900	1730	2451.2	2694.2
10	15	33.05	56.8	200.2	.19910	1745	2401.4	2194.0
11	3	30.65	60.3	111.0	.06575	907	1167	
12	6	32.6	60.05	111.0	.09920	1392	1700	
13	9	32.35	61.2	111.0	.09975	1500	1049	
14	12	32.35	60.05	111.0	.1250	1925	2662	2920
15	15	33.3	57.75	111.0	.1591	2060	2171	2290

Table 5.05 Experimental Data for Heat Transfer to Glycerine (32% by Weight)

Steam Coefficient = $\frac{2500 \text{ KCal}}{\text{hr.m}^2.^\circ\text{C}}$

Sl. No	Liquid Head Pressure psig	Liquid Temperature °C Inlet	Liquid Temperature °C Outlet	Steam Temp. °C	Liquid Flow Rate kg/sec.	U KCal/hr.m².°C	h_i Observed KCal/hr.m².°C	h_i Calculated KCal/hr.m².°C
1.	1	30.75	47.55	104.3	0.311	1228	2413.5	
2.	2	40.90	47.90	103.65	0.492	1277.5	2612.5	2077.0
3.	3	41.85	47.55	103.45	0.506	1350	2355	2494.0
4.	4	41.4	46.15	103.65	0.568	1230	2421.3	2657.4
5.	5	40.9	45.65	103.65	0.634	1593	3146	2933.5
6.	5.5	41.65	46.60	103.45	0.686	1607	4499	
7.	1	41.15	50.10	107.55	0.311	1290	2421.26	
8.	2	42.15	48.0	107.3	0.492	1120	2029.0	2096.1
9.	3	42.6	48.45	106.80	0.506	1323	2019.15	2019.2
10.	4	42.35	47.8	107.3	0.568	1400	3101.82	2644.6
11.	5	42.15	46.85	107.55	0.634	1300	2743.3	2954.0
12.	5.5	42.60	47.05	107.75	0.686	1300	2743.3	
13.	1	42.15	51.75	111.45	0.311	1265	2560.75	
14.	2	42.0	50.1	109.8	0.492	1364.7	3005.2	2139.1
15.	3	43.55	49.65	110.0	0.506	1324.0	2024.65	2550.0
16.	4	43.3	48.7	110.2	0.568	1315.4	2776.0	2690
17.	5	43.3	47.3	110.2	0.634	1065.5	2057	2980.4
18.	5.5	43.75	48.60	110.43	0.686	1275.6	2596.22	
19.	1	42.60	52.0	113.75	0.311	1208.0	2357.5	
20.	2	43.55	49.05	113.75	0.492	1150.0	2062.1	2156.1
21.	3	44.95	51.05	113.73	0.506	1508	2743.3	2455.3
22.	4	44.03	45.65	113.55	0.568	1330	2041.9	2692.1
23.	5	43.77	48.45	113.55	0.634	1248	2492	2820.0
24.	5.5	44.23	49.15	113.75	0.686	1362	2992.1	

Table 5.06 Experimental data for Heat Transfer to Glycerine (62% by weight)

Steam coefficient = 2940 KCal/hr.m^2.^{o}C

Run	Liquid Pressure psig	Liquid Temp. °C Inlet	Liquid Temp. °C Outlet	Steam Temp °C	Liquid Flow Rate kgs/sec.	U KCal/ hr.m^2.^{o}C	h_2 Observed KCal/ hr.m^2 ^{o}C	h_2 Calculated KCal/ hr.m^2.^{o}C
1.	1.	39.47	46.25	97.05	0.298	972	1493	
2.	2	40.7	46.6	97.9	0.4075	2220	1095.6	1541.9
3.	3	42.02	47.95	99.2	0.597	2207	2405.5	2067.6
4.	4	43.07	46.4	102.05	0.615	2240.7	2146.4	2249.4
5.	5	44.72	47.55	102.05	0.756	944.5	1591.5	2734.2
6.								
6.	1	40.45	47.3	101.35	0.298	924.0	1547	
7.	2	42.1	48.7	106.4	0.4075	1902.1	1867.6	
8.	3	42.8	48.45	106.2	0.597	2626.1	3630.5	
9.	4	42.6	47.3	107.3	0.615	2903	2936.0	
20.	5	44.95	48.25	107.10	0.756	2071	1604.5	
21.	1	41.15	48.7	110.0	0.298	900	1295	
22.	2	43.05	49.65	110.4	0.4075	2100	1753.3	1629.5
23.	3	44.25	49.05	109.4	0.597	2918	2690.7	2227.0
24.	4	43.3	48.45	110.65	0.615	2272	2243.3	2279.4
25.	5	45.2	48.7	110.65	0.75	2090	1691.0	2792.8
26.	1	42.1	49.05	113.15	0.298	932.5	1330	
27.	2	44.0	50.60	113.15	0.4075	2070	1603.2	1747.4
28.	3	43.2	51.05	113.75	0.597	2990	2639	2306.1
29.	4	44.95	48.95	113.75	0.615	2209	1981	2296.6
30.	5	46.15	49.65	114.0	0.756	2015	1550.4	2697.03

Table 5.07 Experimental Data for Heat Transfer to Glycerine (55% by weight)

Steam coefficient = 9995 $\frac{kCal}{hr.m^2.^oC}$

Run No.	Liquid Inlet Pressure psig	Liquid Temp. °C Inlet	Liquid Temp. °C Outlet	Steam Temp. °C	Liquid Flow Rate kg/sec.	U $\frac{kCal}{hr.m^2.^oC}$	h_i Observed $\frac{kCal}{hr.m^2.^oC}$	h_i Calculated $\frac{kCal}{hr.m^2.^oC}$
1.	0.5	40.2	45.2	99.05	0.351	754.9	979	
2.	1.0	40.9	45.45	102.2	0.376	709.64	902.6	
3.	2.0	42.4	46.6	99.45	0.492	951.5	1351.6	1311.7
4.	3.0	40.15	44.5	99.65	0.584	1076.4	1559.7	1492.8
5.	4.0	44.25	48.25	101.35	0.666	1183.11	1824.2	1740.1
6.	5.0	45.45	48.7	102.6	0.7725	1105.14	1655.4	1886.7
7.	0.5	40.9	46.15	107.45	0.351	502.0	703.15	
8.	1.0	42.6	47.8	107.95	0.376	742.41	994.17	
9.	2.0	44.7	48.7	107.95	0.492	794.4	1079.0	1451.0
10.	3.0	43.05	47.55	108.15	0.584	1013.62	1536.6	1609.4
11.	4.0	44.25	48.0	106.9	0.666	1020.3	1547.0	1807.7
12.	5.0	47.05	50.8	107.95	0.7725	1192.15	1836	1995
13.	0.5	41.65	47.55	110.65	0.351	761.62	1067.2	
14.	1.0	43.55	48.25	111.65	0.376	667.85	1019.2	
15.	2.0	45.65	49.65	110.4	0.492	760.5	1163.51	
16.	3.0	43.75	48.95	110.4	0.584	1169.6	1788	
17.	4.0	44.95	48.7	110.35	0.666	956.0	1546.9	
18.	5.0	47.55	51.3	110.05	0.7725	1161.64	1875.1	
19.	0.5	43.77	49.65	114.0	0.351	765.0	1128.9	
20.	1.0	44.5	50.1	115.25	0.376	754.9	1183.99	
21.	2.0	46.6	51.5	114.6	0.492	897.22	1487.7	
22.	3.0	44.95	49.4	114.0	0.584	971.8	1572.0	
23.	4.0	45.2	49.15	114.15	0.666	974.6	1577.4	
24.	5.0	40.7	52.25	114.0	0.7725	1034.34	1787.0	

Table 5.08 Experimental Data for Heat Transfer to Water for axial flow

S. No	Water inlet pressure psig	Water Temp. °C Inlet	Water Temp. °C Outlet	Steam Temp. °C	Water Flow Rate kg/sec.	U $\frac{kCal}{hr.m^2.^oC}$	h_i $\frac{kCal}{hr.m^2.^oC}$
1	0.569	34.5	47.05	113.55	0.252	1380	1040
2	0.58	35.65	46.40	113.55	0.426	1520	1565
3	0.62	33.50	40.45	112.95	0.522	1600	1800
4	0.697	33.3	39.9	113.15	0.600	1650	2010
5	0.6975	32.8	38.75	113.55	0.810	1910	2186

Table 5.09 Water data for RPM of Swirl

	Size of tangential entry=1/2"			Size of Tangential entry=3/8"			
S. No.	Pressure Drop kg/cm^2	Air Core Diameter cm.	R.P.M.	S. No.	Pressure Drop kg/cm^2	Air Core Diameter cm.	R.P.M
1	0.141	1.46	1002	1	0.142	1.62	965
2	0.211	1.49	1278	2	0.212	1.529	1220
3	0.282	1.44	1460	3	0.282	1.59	1360
4	0.352	1.46	1607	4.	0.352	1.58	1522

Continued

S. No.	2/8" Tangential Entry			S. No.	1/8" Tangential Entry		
	Pressure Drop kg/cm^2	Air Core Diameter cm.	R.P.M		Pressure Drop kg/cm^2	Air Core Dia. cm.	R.P.M
1.	0.141	1.62	887	1	0.844	1.04	685
2.	0.282	1.62	1360	2	1.0575	1.04	795

Glycerine data for R.P.M of Swirl disc of tangential entry = 1/2 inch.

S.No.	Glycerine 32% by weight			S. No.	Glycerine 42% by weight		
	Pressure Drop kg/cm^2	Air Core Dia. cm.	R.P.M		Pressure Drop kg/cm^2	Air Core Diameter	R.P.M.
1.	0.141	1.46	11022	1	0.141	1.45	1036
2.	0.211	1.49	1315	2	0.211	1.46	1320
3.	0.282	1.44	1490	3	0.282	1.46	1510
4.	0.352	1.46	1640	4	0.352	1.45	1660

S.No.	Glycerine 55% by weight		
	Pressure Drop kg/cm^2	Air Core Diameter cm	R.P.M
1.	0.141	1.49	1050
2.	0.211	1.49	1340
3.	0.282	1.49	1530
4.	0.352	1.49	1685

CHAPTER VI

CONCLUSION AND RECOMMENDATIONS

Studies on heat transfer in swirling flow in long tube has been conducted and liquid film heat transfer coefficient has been calculated based on theoretical considerations. A heat transfer model has been proposed for this system.

In any steam-liquid heat exchanger, major resistance to heat flow is from the liquid film. In this study it has been possible to increase the water film coefficient by 200 percent as compared to film coefficient of axial flow by creating a stabilized swirling flow in the inner pipe by using a swirl chamber and opening the axis of swirl flow to atmosphere. Due to the increase in liquid film coefficient, the overall heat transfer coefficient has also improved by 100 percent. The increase in overall heat transfer coefficient will make it possible to save conveniently about 50 percent heat transfer area for the same duty. A plot showing the extra power consumed to create the swirl flow versus heat transfer area is shown in Fig.6.01.

This reduction in heat transfer will especially be useful when costly alloy tubes for chemical industry have

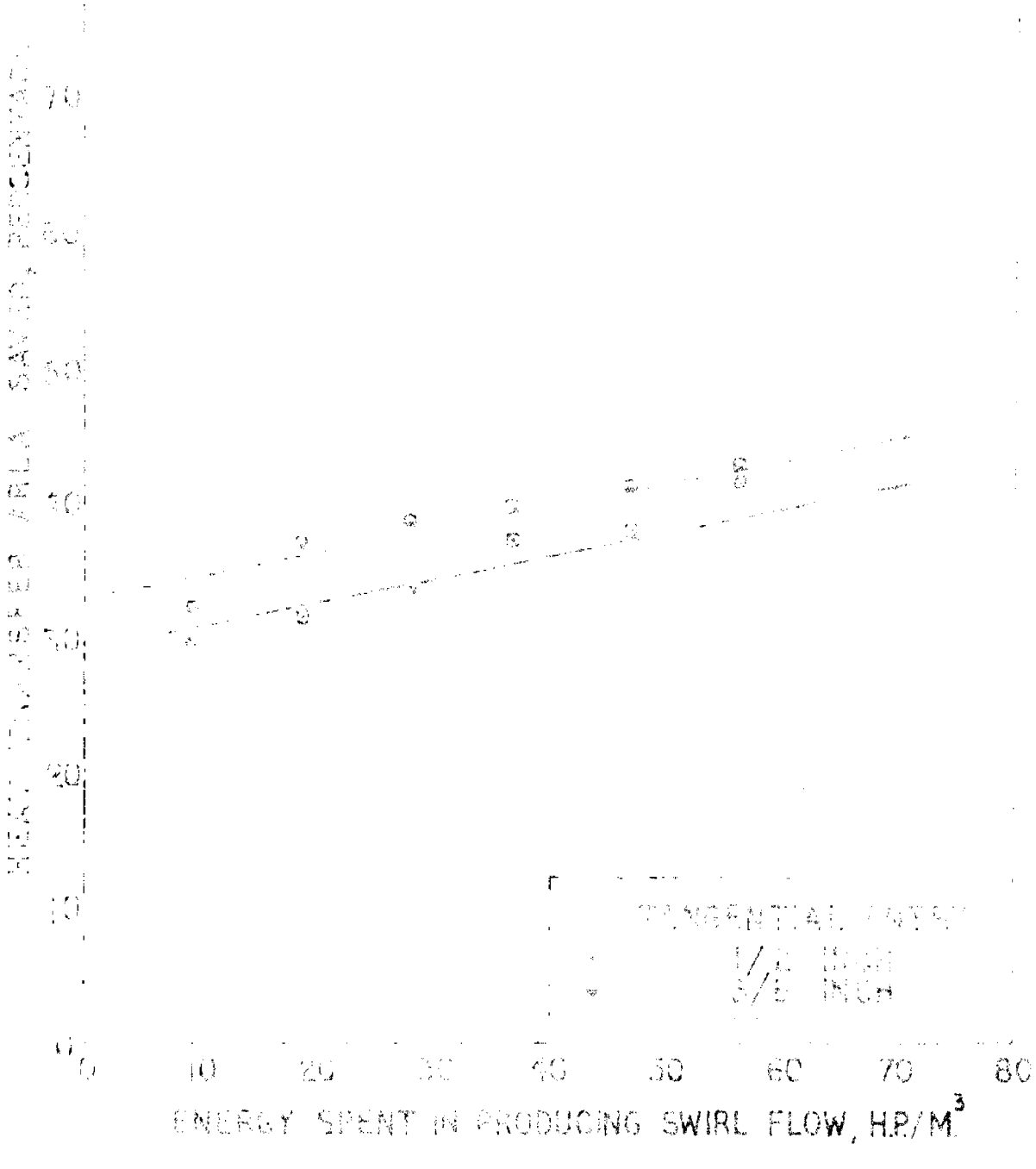

FIG. 3 OR PLOT OF PERCENTAGE SAVING IN HEAT-TRANSFER AREA AGAINST ENERGY CONSUMED IN PRODUCING SWIRL FLOW

to be imposed, availability of which at times becomes difficult for reasons other than economical. Further when the cooling liquid is available under pressure in any process, the liquid can be conveniently led to the heat exchanger through the swirl chamber and thus saving the extra power which has to be consumed for creating swirling flow, at the same time saving heat transfer surface.

Complete study of all the geometric and dynamic parameters is necessary before execution of the equipment is finally established.

APPENDIX A

PHYSICAL PROPERTIES OF GLYCERINE

Table A.1 Physical Properties of Glycerol

Formula: $CH_2OH.CHOH.CH_2OH$, Molecular weight = 92.09

1. Density(12), 100 percent Glycerol

Temp. °C	Density gms./ml.	Temp. °C	Density gms/ml.	Temp. °C	Density gms/ml.
0	1.27269	30.0	1.25512	99.5	1.20970
10	1.26699	40.0	1.24696	220.0	1.20178
15	1.26449	54.0	1.23970	260.0	1.94460
20	1.26194	75.5	1.22560	290.0	1.16721

2. Viscosity of Aqueous Glycerol Solutions(19) Centipoises

Temp °C	Glycerol % Weight						
	0	10	20	30	40	50	60
20	1.005	1.31	1.76	2.50	3.72	6.00	10.0
30	0.8007	1.05	1.35	1.87	2.72	4.21	7.19
40	0.6560	0.826	1.07	1.46	2.07	3.10	5.00
50	0.5094	0.660	0.879	1.16	1.68	2.37	3.76
60	0.4688	0.575	0.731	0.956	1.30	1.86	2.85
70	0.4061	0.500	0.699	0.816	1.08	1.55	2.29
80	0.3565	0.3565	0.3565	0.690	0.930	1.25	1.84
90	0.3165	0.3165	0.3165	0.3165	0.769	1.05	1.52
100	0.2838	0.2838	0.2838	0.2838	0.668	0.910	1.28

3. Specific Heat (14)

ttemp.°C	15	50
C_p $\frac{KCal}{Kg.^oC}$	.576	.576

4. Thermal Conductivity (14)

temp. °C	30	100
K, $\frac{KCal}{hr.m.^oC}$	.0525	0.11

All the physical properties of aqueous glycerine solutions used in calculations have been found out by using linear mixing rule based on pure component.

APPENDIX B

SAMPLE CALCULATIONS

APPENDIX B

B.1 General

Calculation of heat transfer surface

Outside diameter of test section = 31.8 mm

Inside diameter of test section = 30.4 mm

Length of test section = 1143 mm

Heat transfer area = $\pi \times 31.8 \times 10^{-3} \times 1.143$
= 11.43×10^{-2} m^2

B.2 Experimental and Estimated Values of Heat Transfer Coefficient

For Re.10, Table 5.01

Inlet temperature of the water = 99.2°C

Outlet temperature of the water = 44.7°C

Steam temperature = 106.4°C

Mass flow rate of water = 0.666 kg/sec.

Average temperature of the water = 99.95°C

Viscosity of water (μ_b) at average temperature = 0.659 C.P.

Thermal conductivity (k) of water at average temperature = 0.244 KCal/hr.m.°C

Specific heat of water at average temperature = 1 KCal/kg.°C

Temperature difference (ΔT) = 9.5°C

Log mean temperature difference (ΔT_m) = $\dfrac{(T_v - T_i) - (T_v - T_o)}{\ln \dfrac{T_v - T_i}{T_v - T_o}}$

$$= \frac{(106.4 - 99.2) - (106.4 - 44.7)}{\ln \dfrac{106.4 - 99.2}{106.4 - 44.7}} = 66.5°C$$

Overall heat transfer coefficient (U) $= \frac{1x9.5x.606x3600}{11.49x10^{-2}x66.9}$

$= 2670$ KCal/hr.m^2.^{0}C

Steam coefficient from Wilson's plot $= 5830$ KCal/hr.m^2.^{0}C

Experimental liquid film coefficient $= \frac{5830x2670}{(5830-2670)}$

$= 4691$ KCal/hr.m^2.^{0}C

Calculation of Pitot Tube

Diameter of Air Core $= 1.44$ cms.

RPM of Swirl(N) $= 1460$

Area of flow (A) $= \frac{\pi}{4}(D-d)^2 = \frac{\pi}{4}(2.80-1.44)^2$

$= 4.72$ cm^2

Tangential velocity at air core diameter (VTA)

$= \frac{\pi dN}{60} = \frac{\pi x1.44x1460}{60} = 110.6$ cm/sec.

Tangential velocity at the wall radius (VTW)

$= VTA \times \frac{d}{D} = 220.5 \times \frac{1.44}{2.64}$

$= 56$ cms/sec.

Axial velocity (VAX) $= \frac{2.10x1000}{4.72} = 129$ cms/sec.

Average tangential velocity $= \frac{110.5+56}{4.72} = 83.23$ cms/sec.

Actual velocity of the fluid $= \sqrt{(129)^2+(83.29)^2}$

$= 153.9$ cm/sec.

Hydraulic diameter $(D_H) = \frac{4\pi 4.72}{\pi 2.84} = 2.82$ cms

Reynolds Number $= \frac{D_H V_0 \rho}{\mu} = \frac{2.11 \times 153.9 \times [illegible]}{.00659}$

$= 4.9276 \times 10^4$

Friction factor $(f) = \frac{0.079}{(R_e)^{0.25}} = \frac{0.079}{14.9} = 0.0033$

Length of swirl $(L_0) = \frac{\text{Actual velocity}}{\text{Axial velocity}} \times$ length of the tube

$= \frac{153.9}{129.0} \times 114.5 = 353.5$ cms

Pressure drop due to friction in swirl flow $(\Delta P_4) = \frac{4f L_0 V_0^2}{2G_0 D_H}$

$= \frac{4 \times 0.0033 \times 136.5 \times (153.9)^2}{2 \times 981 \times 2.11} = 17.261$ gm/cm^2

Circulation constant (B) = Tangential velocity at aircore dia. $\times$ Air core radius

$= 110.5 \times 0.72 = 79.6$ cm^2/sec.

Radial Pressure drop at the entry head (ΔP_3)

$= \frac{\rho^2}{2G_0} \left[\frac{1}{r^2} - \frac{1}{R^2} \right] = \frac{(79.6)^2}{2 \times 981} \left[\frac{1}{(0.72)^2} - \frac{1}{(1.42)^2} \right]$

$= 4.614$ (illegible) gm/cm^2

Total pressure drop $= \Delta P_3 + \Delta P_4$

$= 21.875$ gm/cm^2 $\simeq 0.022$ kg/cm^2

Friction factor due to total pressure drop $= (\frac{\Delta P}{\rho})_2 \frac{G_0 D_H}{2 L_0 V_0^2} = \frac{.022 \times 981 \times 2.11}{2 \times 196.5 (153.9)^2}$

$= .0033$

Mean axial velocity $(\bar{u}) = \left(\frac{0.606 \times 10^3}{6.35}\right)$

$= 95.5$ cm/sec.

$$\left[1 + \frac{V_\Omega^2}{450\ \bar{u}^2 \ell}\right]^{1/2} = \left[1 + \frac{(153.9)^2}{450(95.5)^2 \times 0.0035}\right]^{1/2}$$

$= 1.346$

$$\frac{D}{D_H} = \frac{2.84}{2.11} = 1.345$$

Calculation of wall temperature (16)

$$T_w = T_a + \frac{h_{io}}{h_{io} + h_o}(T_v - T_a)$$

Steam coefficient from Wilson's plot = 5000 KCal/hr.m^2.^{0}C

Experimental liquid film coefficient = 4031 KCal/hr.m^2.^{0}C

$$h_{io} = h_o \times \frac{\text{Inside diameter of tube}}{\text{outside diameter of tube}}$$

$= 4031 \times \frac{2.84}{3.18} = 4965.22$ KCal/hr.m^2.^{0}C

$T_w = 59.95 + \frac{5060}{10245.22}(106.4 - 59.95) = 70^0$C

Isothermal correction factor $= \left(\frac{\mu_B}{\mu_w}\right)^{0.36} = \left(\frac{0.659}{0.3659}\right)^{0.36}$

$= 1.2366$

Reynolds number for heat transfer $= \frac{D_H G}{\mu}$

$= \frac{0.606 \times 2.11 \times 10^3}{.00659 \times 6.35} = 3.06 \times 10^4$

Prandtl number $= \left(\frac{.00659 \times 360}{0.244}\right) = 9.721$

The theoretical model is

$$Nu = 0.023(Pr)^{1/3}(N_{Re})^{0.8}\left[1+\frac{(V_e)^2}{450\ \bar{u}^2 f}\right]^{1/2}\left(\frac{D}{D_H}\right)\left(\frac{\mu_B}{\mu_w}\right)^{0.36}$$

Calculated Heat Transfer coefficient

$$= h_{i_{cal.}} = \frac{0.023 \times 0.244}{2.11} \times (9.721)^{1/3} \times (3.06 \times 10^4)^{0.8}$$

$$\times 1.346 \times 1.345 \times 1.2566 = 4946.8 \text{ KCal/hr.m}^2.^{\circ}\text{C}$$

$$\text{Percent error} = \frac{h_{i_{exp.}} - h_{i_{cal}}}{h_{i_{exp.}}} \times 100$$

$$= \frac{4891 - 4946.8}{4891} \times 100 = -1.14 \text{ percent}$$

REFERENCES

1. Mace, P.C., and Nissan, A.H., Proceedings Royal Society, A261, 215(1961).

2. Becker, K.M. and Kaye, J. ASME 84 Series C No.2 (1962), 97.

3. Ko, C.Y., Hardcastle, J.L., and Nissan, AIChE Journal, 10(1964), 194.

4. Singh and Ghosh, Transactions Indian Chemical Engineer, Vol.11, No.1-29, 1969.

5. Smithberg and Landis, Transactions ASME Heat Transfer, Twisted Tapes in Horizontal Tubes, C86, 39, 1964.

6. Rao, K.V.A., and Sarma, P.K., Heat Transfer in Forced Convection with Twisted Strips as Swirl Generators, Indian Journal of Technology, Volume 4, Number 6, June 1966.

7. Deissler, R.G., and Perlmutter, M., International Journal Heat and Mass Transfer, 375, 1960.

8. Sharma, B.D., Pamecar, P.S. and Krishna, H.G., Paper presented at the 25th Annual Convention (Silver Jubilee) of Indian Institution of Chemical Engineers held at I.I.T. Delhi (India) 1972.

9. Sharma, B.D., Pamecar, P.S., and Krishna, H.G., Ind. Jr. Tech. 10, 130(1972).

10. Knudsen, J.G., and Katz, D.L., Fluid Dynamics and Heat Transfer, First Edition, McGraw Hill Book Co., Inc., New York, 1958, p.396.

11. Kays, W.M., and London, Compact Heat Exchangers, First Edition, McGraw Hill Book Co., Inc., New York, N.Y., 1958, p.90.

12. Sharma, B.D., Ph.D. Thesis, University of Roorkee, Roorkee, India (In preparation).

13. Newman, A.A., Glycerol, Morgan-Grampian, London, 1968, p.6, 25.

14. Perry, J.H., Chemical Engineers' Handbook, Fourth Edition, McGraw Hill Chemical Engineering Series, p.3-124, 3-204.

15. McCabe, W.L. and Julian, C.S., Unit Operations of Chemical Engineering, Second Edition, McGraw-Hill Book Company, pp.110-113.

16. Kern, D.Q., Process Heat Transfer, International Student Edition, McGraw Hill Book Company, Inc., Tokyo, pp.98.